

ON THE TOPOLOGY OF T-MANIFOLDS OF HIGHER CODIMENSION

ENZO PASQUEREAU

ABSTRACT. This paper undertakes the study of the topology of T-manifolds of arbitrary codimension obtained by combinatorial patchworking with real phase structure as described in [BLdMR24]. We prove new bounds on the number of connected components of T-curves and T-surfaces. For sufficiently high codimension, this improves the results from [BLdMR24].

In addition, we present a new description of patchworking à la Viro for T-manifold of codimension 2. We use this method to construct a family of maximal real algebraic curves in $\mathbb{R}P^3$.

CONTENTS

1. Introduction	2
2. Patchworking of T-manifolds	5
2.1. Real phase structure and T-manifold	5
2.2. Real toric variety	8
3. Real phase structures on the standard simplex	10
3.1. Restrictions and projections of real phase structure	11
3.2. Number of orthants of $\mathcal{E}(\Delta_n)$	13
3.3. Number of simplicial orthants	17
4. Bounds on the number of connected components of T-manifolds	18
4.1. Maximal T-curves	18
4.2. Bounds on the number of connected components of T-curves	22
4.3. Bounds on the number of connected components of T-surfaces	23
5. Construction of k -real phase structures	25
5.1. Stable intersections of real phase structures	25
5.2. Description for T-manifold of codimension 2	27
5.3. Proof of Theorem 5.6	28
5.4. The case of T-curve in dimension 3	34
6. Maximal Curve in codimension 2	35
6.1. Triangulation	35
6.2. Parity code, coloring and orientation	36
6.3. Connected components of C_d	38
6.4. Concluding remarks	44
References	45

Date: February 17, 2026.

2020 *Mathematics Subject Classification.* Primary 14P25, 52B70.

1. INTRODUCTION

Viro's patchworking is a powerful method for constructing real algebraic varieties with prescribed topology [Vir84, Vir06, Ris92]. In its original form, one starts with a collection $(f_i)_i$ of non-degenerate polynomials whose Newton polytope Δ_i form a convex (also known as regular or coherent) subdivision Γ of a polytope Δ . The polynomials f_i are chosen so that the coefficients of common monomials coincide. From this data, Viro's construction produces a real algebraic hypersurface with Newton polytope Δ , whose topology is described as a gluing of the real hypersurfaces defined by the polynomials f_i .

This procedure has proved to be extremely effective in the study of topology of real algebraic varieties. For instance, Viro used it to describe all isotopy types of smooth planar curves of degree 7 [Vir84]. It has also inspired numerous developments and generalizations.

One of these is combinatorial patchworking. It corresponds to the case where the polytopes Δ_i are simplices (i.e. Γ is a triangulation) and where the monomials of each polynomial f_i correspond exactly to the vertices of Δ_i [Ite93, Vir01]. As the name suggests, this method reduces to a combinatorial description, given by a sign distribution on the vertices of the triangulation. The piecewise linear manifold obtained by this procedure is called a T-hypersurface. Here, the assumption of convexity of the triangulation is unnecessary for constructing T-hypersurfaces from the combinatorial description. It remains, however, a key hypothesis to apply Viro's method and deduce an algebraic hypersurface with corresponding topology.

This method has yielded significant advances (including the disproving of Ragsdale conjecture [IV96] and the construction of maximal hypersurfaces [Ite95] [Ite97] [Dem24]). An extension of patchworking to the case of complete intersections has been developed by Sturmfels (for combinatorial patchworking) [Stu94] and then, by Bihan (for general patchworking) [Bih02].

Recently, Renaudineau and Shaw [RS23] proved a conjecture by Itenberg giving an upper bound on the Betti number $b_p(X) := \dim H_p(X; \mathbb{Z}_2)$ of a primitive T-hypersurface X . A triangulation is said to be primitive (or unimodular) when every full-dimensional simplex σ of the triangulation has a lattice volume $\text{Vol}(\sigma)$ of 1. A central concept introduced by Renaudineau and Shaw for their proofs is the one of real phase structure, which reformulates sign distribution.

This result has, since, been generalized in two directions. Firstly, real phase structure have been extended to not only describe patchworks of hypersurfaces but also patchworks of more general varieties [RRS25, RRS22, BLdMR24].

Another generalization arose from forgetting the convexity of the triangulation. Indeed, combinatorial patchworking has been reinterpreted in the framework of tropical geometry, where primitive convex triangulations become non-singular tropical hypersurfaces. This geometric point of view provides new intuition and additional tools notably tropical homology. However, going back to triangulation, Brugallé, López de Medrano, and Rau [BLdMR24] proved that the inequalities still hold without any convexity assumption.

Theorem 1.1 ([BLdMR24]). *Let X be a T-manifold of codimension k with a smooth Newton polytope Δ . Then,*

$$(1) \quad \forall p \geq 0, \quad b_p(X) \leq \sum_{q=0}^{n-k} h^{p,q}(Y_\Delta^k)$$

where Y_Δ^k denotes a smooth complete intersection of k hypersurfaces with Newton polytope Δ in the toric variety $\mathbb{C}X_\Delta$ associated to Δ and $h^{p,q}(Y_\Delta^k)$ is its (p,q) -Hodge number.

We refer to Section 2 for precise definitions of T-manifolds, real phase structures and smooth polytopes.

In the setting of Renaudineau and Shaw, a T-hypersurface is homeomorphic to the real part $\mathbb{R}X$ of a smooth algebraic hypersurface $\mathbb{C}X$ with Newton polytope Δ . In this case, the sum of all the Betti numbers satisfies the Smith-Thom inequality:

$$\sum_{p \geq 0} b_p(\mathbb{R}X) \leq \sum_{p \geq 0} b_p(\mathbb{C}X)$$

A real algebraic variety attaining this bound is said to be maximal. Without convexity and in higher codimension, no homeomorphism is known in general between T-manifold and any algebraic variety. Still, by analogy with real algebraic geometry, we adopt the following terminology.

Definition 1.2.

A T-manifold for which the inequalities (1) are equalities for each p is called **maximal**.

Let Δ be a polytope and k an integer. For any $d \geq 1$, let X_d be a T-manifold of codimension k with Newton polytope the dilation $d\Delta$. We say the family $(X_d)_{d \geq 1}$ is **asymptotically maximal** on Δ if

$$\forall p \geq 0, b_p(X_d) \sim_{d \rightarrow \infty} \sum_q h^{p,q}(Y_{d\Delta}^k).$$

T-hypersurfaces have been studied for almost thirty years, and many examples of maximal T-hypersurfaces ([Ite95, Ite97, Dem24]) and asymptotically maximal families of T-hypersurfaces ([IV07, Ber02]) have been constructed. In contrast, since their definition is more recent, not much is known for T-manifolds of higher codimension.

The present paper explores this new setting. We are interested in "extremal" T-manifolds with large Betti numbers, and in particular, on the number of connected components.

We establish two new upper bounds on the number of connected components for T-curves and T-surfaces.

Theorem 1.3. *Let Δ be a smooth lattice polytope of dimension n .*

- *A T-curve X with Newton polytope Δ satisfies:*

$$b_0(X) \leq \frac{n+1}{3} \text{Vol}(\Delta)$$

- *A T-surface X with Newton polytope Δ satisfies:*

$$b_0(X) \leq \frac{7n^2 + 5n + 12}{30} \text{Vol}(\Delta)$$

We also compute the following asymptotic of the right-hand side of (1), when $p = 0$:

Lemma 1.4. *The sum $\sum_{q=0}^{n-k} h^{0,q}(Y_{d\Delta}^k)$ is a polynomial in d whose leading term is*

$$\frac{k!}{n!} \binom{n}{k} \text{Vol}(\Delta) d^n,$$

where $\{n\}_k$ denotes the Stirling number of the second kind.

Comparing these two results yields the following result on the asymptotic maximality of T-manifolds:

Corollary 1.5. *Let Δ be a smooth lattice polytope of dimension n .*

- *If $n \geq 6$, there is no asymptotically maximal family of T-curves on Δ .*
- *If $n \geq 65$, there is no asymptotically maximal family of T-surfaces on Δ .*

For T-curves, an additional obstruction to maximality arises from the planarity of the dual graph of the triangulation. This yields even stronger restrictions:

Theorem 1.6. *Let Δ be a smooth lattice polytope of dimension n . If $n \geq 4$ and $d \geq n+1$, there is no maximal T-curve with Newton polytope $d\Delta$.*

Real phase structures, and thus T-manifolds, are more abstruse to describe than sign distributions and T-hypersurfaces. Even the existence of real phase structure on a given unimodular triangulation is not immediately clear.

In a second part of this text, we introduce a new method for constructing real phase structures. Given an orientation of the edges of a triangulation and two real phase structures, we describe a new real phase structure. The associated T-manifold can be interpreted as a combinatorial equivalent of real stable intersections in tropical geometry (see [MS15, Section 4.3] for background on stable intersections).

This construction provides:

Theorem 1.7. *Let Γ be a triangulation of Δ . For any k between 0 and n , there exists a k -real phase structure on Γ .*

This combinatorial real stable intersection is particularly well-suited for codimension 2, since the description of real phase structures for T-hypersurfaces reduces to sign distributions. This yields a combinatorial description of a subclass of T-manifolds of codimension 2 reminiscent of classical combinatorial patchworking.

Combined with Sturmfels' method, we show a realizability criterion ensuring that the resulting T-manifolds have the topology of smooth complete intersections.

Theorem 1.8. *Let Δ be a smooth lattice polytope, Γ be a convex triangulation of Δ , \mathcal{O} an acyclic orientation of Γ and two sign distributions μ_1, μ_2 . Consider the T-hypersurface $X_{\mathcal{E}_{\mu_1}}$ and the T-manifold $X_{\mathcal{E}_{\mu_1} \cap \mathcal{O} \mathcal{E}_{\mu_2}}$ of codimension 2. There exists two transverse real algebraic hypersurfaces H_1 and H_2 with Newton polytope Δ in $\mathbb{R}X_\Delta$ such that the triple $(\tilde{\Delta}, X_{\mathcal{E}_{\mu_1}}, X_{\mathcal{E}_{\mu_1} \cap \mathcal{O} \mathcal{E}_{\mu_2}})$ is homeomorphic to $(\mathbb{R}X_\Delta, H_1, H_1 \cap H_2)$.*

Using this description we explicitly construct maximal T-curves in $\mathbb{R}P^3$.

Theorem 1.9. *For each integer $d \geq 1$, there exists a pair (Σ_d, C_d) where Σ_d is a maximal T-surface and C_d a maximal T-curve both with Newton polytope $d\Delta_3$ such that $C_d \subset \Sigma_d$. The triple $(\tilde{d\Delta}_3, \Sigma_d, C_d)$ is homeomorphic to $(\mathbb{R}P^3, H_1, H_1 \cap H_2)$ where H_1 and H_2 are transverse maximal real algebraic hypersurfaces of degree d .*

Here $d\Delta_3$ is the tetrahedron with vertices $(0, 0, 0)$, $(d, 0, 0)$, $(0, d, 0)$ and $(0, 0, d)$.

Note that the pair $(H_1, H_1 \cap H_2)$ is not maximal.

Organization of the paper.

- In Section 2, we present the construction of T-manifolds via real phase structures as presented in [BLdMR24].

- Section 3 is devoted to a local study of real phase structures, which provides the key technical ingredients needed for our later results.
- In Section 4, we establish our results on the number of connected components of T-curves and T-surfaces.
- Section 5 introduces a construction of real phase structures and its application to T-manifolds of codimension 2.
- In Section 6, we apply this method to construct a family of maximal T-curves in the three-dimensional projective space.

Acknowledgments. We are deeply grateful to Erwan Brugallé for his guidance, for many insightful discussions, and for his helpful suggestions and advice during the preparation of this work.

2. PATCHWORKING OF T-MANIFOLDS

2.1. Real phase structure and T-manifold. We begin by defining T-manifold following [BLdMR24]. For T-hypersurfaces, this construction has first been described by Renaudineau and Shaw in the context of tropical geometry [RS23].

Let $\Delta \subset \mathbb{R}^n$ be a full-dimensional convex polytope with vertices in the lattice \mathbb{Z}^n . Such polytopes are referred to as lattice polytopes. Consider a triangulation Γ of Δ with vertices in \mathbb{Z}^n . We denote by $F_k(\Gamma)$ the set of k -simplices of Γ , and for a simplex τ , we denote by $F_k(\tau)$ the set of its k -faces. A simplex with vertices v_0, v_1, \dots, v_k will be denoted by $[v_0, v_1, \dots, v_k]$. We suppose throughout the text that Γ is unimodular meaning that all simplices of $F_n(\Gamma)$ have euclidean volume $\frac{1}{n!}$. The lattice volume of a full-dimensional lattice polytope $\Delta \subset \mathbb{R}^n$, denoted by $\text{Vol}(\Delta)$, is the euclidean volume of Δ divided by $\frac{1}{n!}$ the volume of a unimodular simplex.

For each simplex σ , we define its integral tangent space $T(\sigma) \subset \mathbb{Z}^n$ as the sub-lattice spanned by the differences of two points of $\sigma \cap \mathbb{Z}^n$. We denote by $T_2(\sigma) := T(\sigma) \otimes \mathbb{F}_2 \subset \mathbb{F}_2^n$ and $T_2^\perp(\sigma) \subset (\mathbb{F}_2^n)^\vee = \text{Hom}(\mathbb{F}_2^n, \mathbb{F}_2)$ the orthogonal of $T_2(\sigma)$ in the dual of \mathbb{F}_2^n . We suppose throughout the text that Δ is smooth, that is for any vertex v of Δ , there is a decomposition $\mathbb{Z}^n = \bigoplus T(\rho)$, where the sum runs over all the edges ρ of Δ incident to v .

Fix an affine space \mathcal{Q}^n directed by $(\mathbb{F}_2^n)^\vee$. We will identify \mathcal{Q}^n with the set $\{+, -\}^n$ of orthant of \mathbb{R}^n , so the action of $(\mathbb{F}_2^n)^\vee$ on \mathcal{Q}^n corresponds to the one of the reflection group generated by reflections across the coordinate hyperplanes.

Definition 2.1. A real phase structure \mathcal{E} on the k -skeleton of Γ is a choice for each $\sigma \in F_k(\Gamma)$ of an affine subspace $\mathcal{E}(\sigma)$ of \mathcal{Q}^n directed by $T_2^\perp(\sigma)$ satisfying the following **parity condition**: for each $\tau \in F_{k+1}(\Gamma)$ and $s \in \mathcal{Q}^n$ there is an even number of $\sigma \in F_k(\tau)$ such that $s \in \mathcal{E}(\sigma)$.

We also call \mathcal{E} a k -real phase structure on Γ .

Example 2.2. Consider the triangle $\Delta_2 = [a, b, c]$ with vertices $a = (0, 0), b = (1, 0), c = (0, 1)$. We endowed it with its trivial (and unique triangulation). A real phase structure \mathcal{E}_1 on the 1-skeleton of Δ_2 is given by

- $\mathcal{E}_1([a, b]) = \{(+, +), (+, -)\}$
- $\mathcal{E}_1([a, c]) = \{(+, +), (-, +)\}$
- $\mathcal{E}_1([b, c]) = \{(+, -), (-, +)\}$

In the following, given a simplex τ of Γ , we denote by $\mathcal{E}(\tau) = \bigcup_{\sigma \in F_k(\tau)} \mathcal{E}(\sigma)$.

Given a real phase structures on the k -skeleton of Γ , we define a PL manifolds called T-manifolds by the following construction.

For each $s \in \mathcal{Q}^n$, consider a copy $s(\Delta)$ of Δ with the triangulation $s(\Gamma)$, which is a copy of Γ . We say that $s(\Delta)$ is the symmetric copy of Δ in the orthant s .

We form a topological space gluing together the $s(\Delta)$ on their faces. For each face F of Δ , we identify the face $s(F)$ and $t(F)$ each time that $t - s \in T_2^\perp(F)$. The resulting space is denoted by $\tilde{\Delta}$, and it is triangulated by the extended triangulation $\tilde{\Gamma}$ obtained by the gluing of the copies $s(\Gamma)$.

Let $\text{Bar}(\tilde{\Gamma})$ be the barycentric subdivision of $\tilde{\Gamma}$. The vertices v_σ of $\text{Bar}(\tilde{\Gamma})$ are the barycenter of the simplex σ of $\tilde{\Gamma}$. For a simplex $\tau \in \Gamma$ and an orthant $s \in \mathcal{Q}^n$, we associate to the simplex $s(\tau)$ of $\tilde{\Gamma}$ the subspace $C_{\mathcal{E}}(s(\tau))$ defined as the full subcomplex of $\text{Bar}(\tilde{\Gamma})$ whose vertices are the barycenters $v_{s(\sigma)}$ of the faces of $s(\sigma)$ of $s(\tau)$ such that $s \in \mathcal{E}(\sigma)$. Each subcomplex $C_{\mathcal{E}}(s(\tau))$ can be made of several simplices of $\tilde{\Gamma}$ or empty if $s \notin \mathcal{E}(\tau)$.

Example 2.3. This construction is illustrated in the simple case of Example 2.2 in Figure 1. On the top left, the four symmetric copies of Δ_2 appear in their corresponding quadrant. On the top right, we obtain $\tilde{\Delta}_2$ by gluing these four copies together. The boundary edges must be identified according to the arrows. At the bottom, the barycentric subdivision of $\tilde{\Delta}_2$ is shown (the identification of the boundary edges is not shown). For the triangle $\tau = \Delta_2$, if $s \in \mathcal{E}_1(\Delta_2)$, the corresponding subcomplex $C_{\mathcal{E}_1}(s(\tau))$ is drawn in green. It is made of two edges and three vertices of the barycentric subdivision $\text{Bar}(s(\Delta_2))$. For an edge γ of Δ_2 , if $s \in \mathcal{E}_1(\gamma)$, the corresponding 0-cell $C_{\mathcal{E}_1}(s(\gamma))$ is circled in a darker green.

Definition 2.4. A regular cell complex subdividing a topological space X is a finite set \mathcal{C} of topological closed balls (called cells) in X satisfying:

- the interiors $\dot{\sigma}$ of the cells $\sigma \in \mathcal{C}$ partition X
- the boundary $\partial\sigma$ of a cell $\sigma \in \mathcal{C}$ is a union of cells of \mathcal{C}

The underlying space $|\mathcal{C}|$ of a cell complex \mathcal{C} is the topological space X .

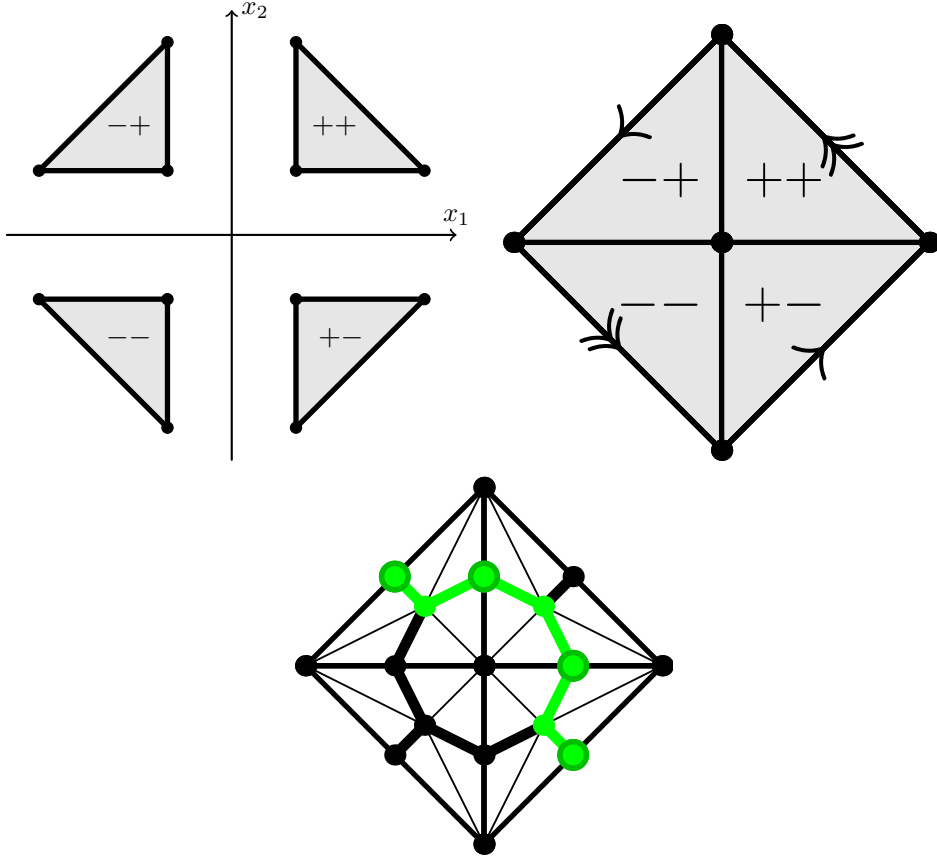
Proposition 2.5 (Proposition 4.11, [BLdMR24]). *The collection of all the of the $C_{\mathcal{E}}(\tau)$, for $\tau \in \tilde{\Gamma}$, defines a regular cell complex. The m -cells of this complex are precisely the $C_{\mathcal{E}}(s(\tau))$ where τ is a $(m+k)$ -simplex of Γ and $s \in \mathcal{E}(\tau)$. The underlying space $X_{\mathcal{E}}$ of this cell decomposition is a PL manifold of dimension $n - k$ and the cells $C_{\mathcal{E}}(\sigma)$ are PL balls.*

The space $X_{\mathcal{E}}$ is the T-manifold associated to the real phase structure \mathcal{E} , and we refer to the above decomposition as the canonical cell decomposition of $X_{\mathcal{E}}$. By construction, we have $C_{\mathcal{E}}(s(\tau)) = X_{\mathcal{E}} \cap s(\tau)$, for any simplex τ of Γ and orthant $s \in \mathcal{Q}^n$ such that $s \in \mathcal{E}(\tau)$.

Definition 2.6. Let Δ be a lattice polytope. A T-manifold of codimension k with Newton polytope Δ is a T-manifold $X_{\mathcal{E}}$, where \mathcal{E} is a real phase structure on the k -skeleton of a triangulation of Δ .

Example 2.7. The T-curve $X_{\mathcal{E}_1}$ with Newton polytope Δ_2 , from Example 2.2, is represented in Figure 1.

Example 2.8. For any 0-simplex (i.e. vertex) v , we have $T_2^\perp(v) = (\mathbb{F}_2^n)^\vee$. Thus, for any lattice polytope Δ and triangulation Γ , there is always a unique real phase

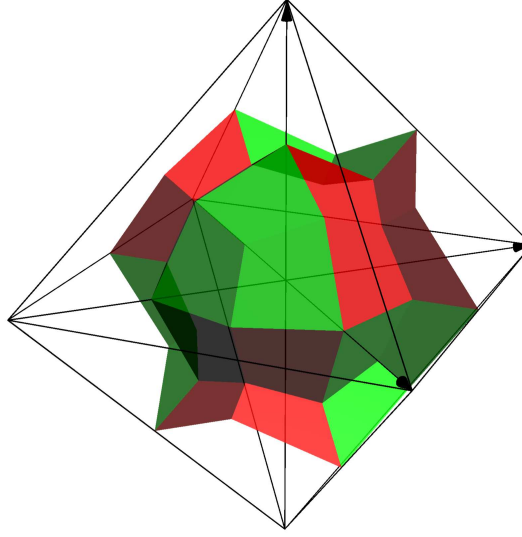
FIGURE 1. The construction of $\tilde{\Delta}_2$ the T-curve associated to \mathcal{E}_1

structure \mathcal{E}_0 on the 0-skeleton of Γ . It is defined by $\mathcal{E}_0(v) = \mathcal{Q}^n$. The parity condition is well satisfied since for any edge $[v, v']$ of Γ , we have $\mathcal{E}_0(v) = \mathcal{E}_0(v')$. It follows, that independently of Γ , the T-manifold $X_{\mathcal{E}_0}$ is always the full space $\tilde{\Delta}$. Furthermore, the canonical cell decomposition is exactly the subdivision $\tilde{\Gamma}$.

Example 2.9. For $\Delta_3 = [a, b, c, d]$ with vertices $a = (0, 0, 0)$, $b = (1, 0, 0)$, $c = (0, 1, 0)$ and $d = (0, 0, 1)$, a real phase structure \mathcal{E}_2 on the 1-skeleton of Δ_3 is given by

- $\mathcal{E}_2([a, b]) = \{(+, +, +), (+, -, +), (+, +, -), (+, -, -)\}$
- $\mathcal{E}_2([a, c]) = \{(+, -, +), (-, -, +), (+, -, -), (-, -, -)\}$
- $\mathcal{E}_2([a, d]) = \{(+, +, +), (-, +, +), (+, -, +), (-, -, +)\}$
- $\mathcal{E}_2([b, c]) = \{(+, +, +), (+, +, -), (-, -, +), (-, -, -)\}$
- $\mathcal{E}_2([b, d]) = \{(-, +, +), (-, -, +), (+, +, -), (+, -, -)\}$
- $\mathcal{E}_2([c, d]) = \{(+, +, +), (-, +, +), (+, -, -), (-, -, -)\}$

The T-surface $X_{\mathcal{E}_2}$ is represented in Figure 2. On this representation, the opposite faces of the octahedron need to be identified.

FIGURE 2. The T-surface $X_{\mathcal{E}_2}$ of Example 2.9

Example 2.10. For $\Delta_3 = [a, b, c, d]$ with vertices $a = (0, 0, 0)$, $b = (1, 0, 0)$, $c = (0, 1, 0)$ and $d = (0, 0, 1)$, a real phase structure \mathcal{E}_3 on the 2-skeleton of Δ_3 is given by

- $\mathcal{E}_3([a, b, c]) = \{(+, +, +), (+, +, -)\}$
- $\mathcal{E}_3([a, b, d]) = \{(+, +, +), (+, -, +)\}$
- $\mathcal{E}_3([a, c, d]) = \{(+, +, -), (-, +, -)\}$
- $\mathcal{E}_3([b, c, d]) = \{(+, -, +), (-, +, -)\}$

The T-curve $X_{\mathcal{E}_3}$ is represented in Figure 3. On this representation, the opposite faces of the octahedron need to be identified.

Example 2.11. In codimension 1, a real phase structure is equivalently defined by a sign distribution $\mu: F_0(\Gamma) \rightarrow \{-, +\}$ on the vertices of Γ . Such a sign distribution μ extends to vertices of $\tilde{\Gamma}$ by the following rule:

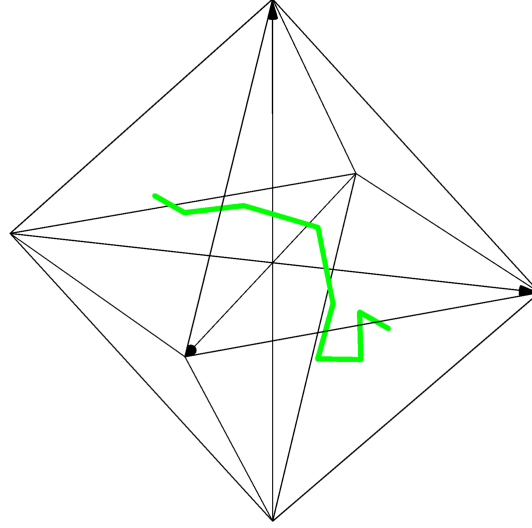
$$\mu(s(v)) = (-1)^{s \cdot v} \mu(v)$$

where $s \cdot v = \sum_{i=1}^n s_i v_i$. We then define \mathcal{E}_μ by saying that $s \in \mathcal{E}_\mu([a, b])$ if and only if $\mu(s(a)) \neq \mu(s(b))$.

For any sign distribution μ , we obtain a 1-real phase structure \mathcal{E}_μ . Conversely, a real phase structure of codimension 1 determines, up to inversion of all the signs, a sign distribution $\mu: F_0(\Gamma) \rightarrow \{-, +\}$. See [BLdMR24, Example 4.3] for the details of this bijection.

For example, the real phase structure \mathcal{E}_1 , of example 2.7, arises from the sign distribution μ (or $-\mu$), where μ is defined by $\mu(a) = +$, $\mu(b) = -$ and $\mu(c) = -$.

2.2. Real toric variety. In this subsection, we relate the construction of T-manifolds of codimension 0 and 1 to real algebraic geometry.

FIGURE 3. The T-curve X_{E_3} of Example 2.10

For a lattice polytope Δ of \mathbb{R}^n with lattice points $\Delta \cap \mathbb{Z}^n = \{m_0, \dots, m_N\}$, we can define an application

$$\begin{aligned} \phi_{\Delta}^n: \quad & (\mathbb{C}^*)^n \longrightarrow \mathbb{C}P^N \\ & (t_1, \dots, t_n) \longmapsto [t^{m_0} : \dots : t^{m_N}] \end{aligned}$$

where $[u_0 : u_1 : \dots : u_N]$ are the homogeneous coordinates on $\mathbb{C}P^N$ and $t^{m_i} := t_1^{m_{i,1}} \dots t_n^{m_{i,n}}$.

Denote by $\mathbb{C}\mathring{X}_{\Delta}$ the image of ϕ_{Δ} . The Zariski closure of the image $\mathbb{C}\mathring{X}_{\Delta}$ in $\mathbb{C}P^N$ is the complex toric variety $\mathbb{C}X_{\Delta}$.

Example 2.12. For the standard n -simplex

$$\Delta_n = \{x \in \mathbb{R}^n \mid x_i \geq 0 \text{ and } x_1 + \dots + x_n \leq 1\},$$

the image $\mathbb{C}\mathring{X}_{\Delta_n}$ is the complement $\{[u_0 : \dots : u_n] \mid u_i \in \mathbb{C}^*\}$ of the coordinate hyperplanes in $\mathbb{C}P^n$ and its Zariski closure in $\mathbb{C}P^n$ is

$$\mathbb{C}X_{\Delta_n} = \mathbb{C}P^n.$$

Remark 2.13. For any positive integer m , we denote by $m\Delta$ the m -dilation $\{mx \mid x \in \Delta\}$ of Δ . A polytope and its dilations have isomorphic (as algebraic varieties) toric varieties: $\mathbb{C}X_{m\Delta} = \mathbb{C}X_{\Delta}$.

For a face F of Δ with $M+1$ lattice points, we can see $\mathbb{C}P^M$ as the subset $\{[u_0 : \dots : u_N] \mid u_i = 0 \text{ if } m_i \notin F \cap \mathbb{Z}^n\}$ of $\mathbb{C}P^N$. This defines an embedding $\mathbb{C}X_F \hookrightarrow \mathbb{C}X_{\Delta}$. More precisely, we have the stratification $\mathbb{C}X_{\Delta} = \bigcup_{F \text{ face of } \Delta} \mathbb{C}\mathring{X}_F$.

Lemma 2.14 (Theorem 2.4.3,[CLS11]). *The toric variety $\mathbb{C}X_{\Delta}$ is smooth if and only if the polytope Δ is smooth.*

The real part of the toric variety $\mathbb{C}X_{\Delta}$ is denoted $\mathbb{R}X_{\Delta}$ and is defined as the intersection of $\mathbb{C}X_{\Delta}$ with $\mathbb{R}P^N \subset \mathbb{C}P^N$.

Theorem 2.15 (Theorem 5.3 and 5.4, Chapter 11, [GKZ08]). *There is a homeomorphism from $\tilde{\Delta}$ to the real part $\mathbb{R}X_{\Delta}$. This homeomorphism is stratified in the following sense: for any face F of Δ , the gluing $\tilde{F} \subset \tilde{\Delta}$ is sent to $\mathbb{R}X_F \subset \mathbb{R}X_{\Delta}$. In addition, for $s \in \mathcal{Q}^n$, the copy $s(\Delta)$ is sent to the orthant*

$$\mathbb{R}X_{\Delta} \cap \{[u_0 : \dots : u_N] \mid \forall i, s_i u_i \geq 0\}$$

associated to s .

It follows from Example 2.8 that T-manifolds of codimension 0 are toric varieties:

Corollary 2.16. *Let Δ be a lattice polytope, let Γ be a triangulation of Δ , and let \mathcal{E} a real phase structure on the 0-skeleton of Γ , then $X_{\mathcal{E}}$ is homeomorphic to $\mathbb{R}X_{\Delta}$.*

For a map $\nu: \Delta \cap \mathbb{Z}^n \rightarrow \mathbb{R}$, define the polyhedron

$$\Delta_{\nu} = \text{Conv}\{(x, h) \in (\Delta \cap \mathbb{Z}^n) \times \mathbb{R} \mid h \geq \nu(x)\} \subset \mathbb{R}^{n+1}.$$

The orthogonal projection of the bounded faces of Δ_{ν} on Δ defines a subdivision Γ_{ν} of Δ . Subdivisions obtained in this way are called convex (or regular, or coherent).

The relationship between algebraic geometry and patchworking comes from Viro's theorem. Here we reformulate it in terms of real phase structures.

Theorem 2.17 (Viro's theorem [Vir84]). *If Γ_{ν} is a convex triangulation on Δ and \mathcal{E} a 1-real phase structure on Γ_{ν} , there exists an algebraic hypersurface H of $\mathbb{R}X_{\Delta}$ such that the pair $(\mathbb{R}X_{\Delta}, H)$ is homeomorphic to $(\tilde{\Delta}, X_{\mathcal{E}})$. This homeomorphism is stratified in the sense of Theorem 2.15.*

If μ is a sign distribution corresponding to \mathcal{E} (see Example 2.11), the hypersurface H is given by the polynomial equation $\{P_t = 0\} \subset \mathbb{R}X_{\Delta}$, for sufficiently small $t > 0$, where

$$P_t(x) = \sum_{a \in F_0(\Gamma_{\nu})} \mu(a) t^{\nu(a)} x^a.$$

Such a polynomial is called a *Viro polynomial*.

3. REAL PHASE STRUCTURES ON THE STANDARD SIMPLEX

The goal of this section is to prove the two following theorems.

Theorem 3.1. *Let Δ be a lattice polytope of dimension n , let Γ be an unimodular triangulation of Δ and let \mathcal{E} be a real phase structure on the k -skeleton of Γ . The number of maximal cells in the canonical cell decomposition of $X_{\mathcal{E}}$ is*

$$\sum_{i=k}^n \binom{n}{k} \text{Vol}(\Delta).$$

Theorem 3.2. *Let Δ be a lattice polytope of dimension n , let Γ be an unimodular triangulation of Δ and let \mathcal{E} be a real phase structure on the k -skeleton of Γ . The number of maximal and simplicial cells in the canonical cell decomposition of $X_{\mathcal{E}}$ is at most*

$$\frac{2}{k+1} \binom{n+1}{k} \text{Vol}(\Delta).$$

Here an m -cell is said simplicial if it has exactly $m + 1$ facets.

Recall that a full-dimensional simplex $\sigma \in \Gamma$ contributes to a full-dimensional cell $C_{\mathcal{E}}(s(\sigma))$ of $X_{\mathcal{E}}$ for each orthant $s \in \mathcal{E}(\sigma)$. Thus, we will enumerate the orthants of $\mathcal{E}(\sigma)$ for σ a unimodular simplex.

In this section, the lattice polytope Δ considered is a unimodular lattice simplex of dimension n in \mathbb{R}^n , and \mathcal{E} denotes a real phase structure on the k -skeleton of Δ . Up to a unimodular transformation, one can always choose the standard n -simplex $\Delta_n = \text{Conv}(0, e_1, \dots, e_n) \subset \mathbb{R}^n$ where (e_1, \dots, e_n) is the canonical basis of \mathbb{R}^n . The polytope Δ_n has a unique triangulation, whose simplices are precisely the faces of Δ_n .

In the dual setting of fans, real phase structures have been studied in [RRS22]. In particular, it was shown there that real phase structures on a fan are in bijection with the orientations of the matroid associated to the fan. By the topological representation theorem of Folkman and Lawrence [FL78], every oriented matroid is realizable by arrangement of pseudohyperplanes in a real projective space.

The arrangement corresponding to a real phase structure \mathcal{E} can be recovered from the associated T-variety $X_{\mathcal{E}} \subset \widetilde{\Delta}_n$: For each facet F of Δ , \widetilde{F} intersects $X_{\mathcal{E}}$ as a hypersurface H_F in $X_{\mathcal{E}}$. It turns out that the collection of the H_F in $X_{\mathcal{E}}$ defines an arrangement of pseudohyperplanes in a projective space. In particular, the T-manifold $X_{\mathcal{E}}$ is homeomorphic to $\mathbb{R}P^{n-k}$.

This provides the following geometrical intuition of real phase structures on unimodular simplex: the structure \mathcal{E} can be thought as an arrangement \mathcal{A} of $n + 1$ (pseudo)hyperplanes in $\mathbb{R}P^{n-k}$. The chambers (i.e. the full-dimensional region) c of the arrangement \mathcal{A} correspond to orthants $s \in \mathcal{E}(\Delta_n)$, and the vertices of the chambers c correspond to k -faces σ of Δ_n such that $s \in \mathcal{E}(\sigma)$.

The Figure 4 represents the arrangement of four pseudolines in $\mathbb{R}P^2$ obtained from the real phase structure \mathcal{E}_2 of Example 2.9. Each of the four black lines corresponds to a facet of Δ_3 , and they delimit seven chambers corresponding to the non-empty orthants of $X_{\mathcal{E}_2}$.

With this correspondence, estimating the number of orthants in $\mathcal{E}(\Delta)$ is equivalent to counting the chambers in a pseudohyperplanes arrangement. The answer of this problem is well known in the theory of oriented matroids. However, we are here only interested to the simple case of uniform matroids. Thus, to keep the presentation self-contained and to avoid relying on the full machinery of oriented matroids and topological representation theory, we prefer to use direct combinatorial arguments based on the elementary properties of real phase structures.

3.1. Restrictions and projections of real phase structure. For a facet F of Δ_n , the orthogonal space $T_2^\perp(F)$ is a one-dimensional \mathbb{F}_2 -vector space. We denote its unique non-zero element by e_F . Since Δ_n is a unimodular simplex, it follows that for any strict subset $I \subsetneq F_{n-1}(\Delta_n)$, the vectors $(e_F)_{F \in I}$ are linearly independent. The only non-trivial relation between the $(e_F)_{F \in F_{n-1}(\Delta_n)}$ is:

$$\sum_{F \in F_{n-1}(\Delta_n)} e_F = 0.$$

Given a lattice simplex, the quotient $\mathcal{Q}^n/T_2^\perp(\sigma)$ is an affine space of direction the dual space $T_2^\vee(\sigma) = \text{Hom}(T_2(\sigma), \mathbb{F}_2)$, since this vector space is canonically isomorphic to the quotient $(\mathbb{F}_2^n)^\vee/T_2^\perp(\sigma)$. Let $\pi_\sigma: \mathcal{Q}^n \rightarrow \mathcal{Q}^n/T_2^\perp(\sigma)$ be the projection map.

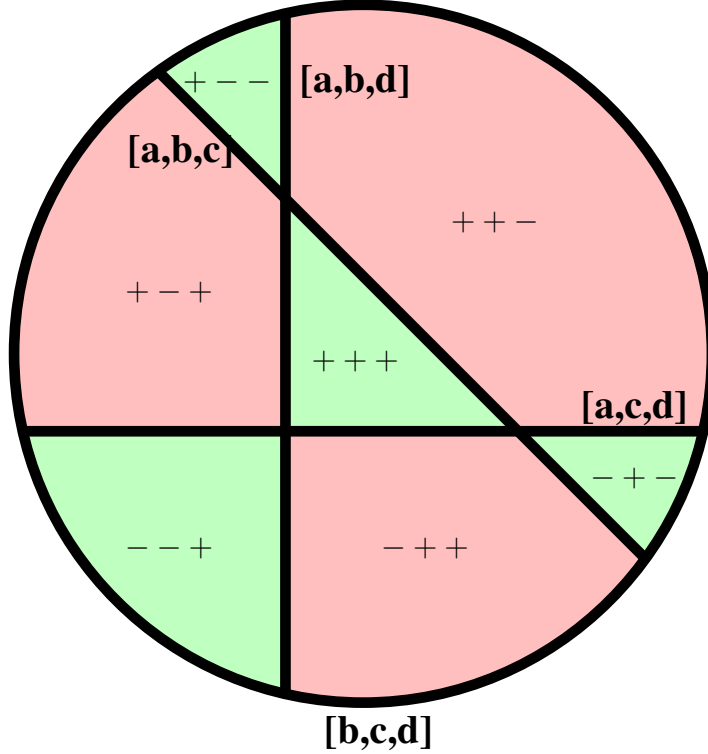


FIGURE 4. Arrangement of pseudolines in $\mathbb{R}P^2$ associated to \mathcal{E}_2

Definition 3.3. Let \mathcal{E} be a real phase structure on the k -skeleton of Δ_n and let F be a facet of Δ_n .

If $k < n$, the restriction $\mathcal{E}|_F$ is defined by $\mathcal{E}|_F(\sigma) = \pi_F(\mathcal{E}(\sigma))$ for each k -simplex σ of F .

If $k > 0$, the projection \mathcal{E}^F is defined by $\mathcal{E}^F(\sigma \cap F) = \pi_F(\mathcal{E}(\sigma))$ for each k -simplex σ of Δ_n not contained in F .

The restriction and projection operations on real phase structure are the equivalent of deletion and contraction for (oriented) matroids. In the case of real phase structure on fan, they are defined and studied in [RRS25].

Proposition 3.4. Let \mathcal{E} be a real phase structure on the k -skeleton of Δ_n , and let F be a facet of Δ_n .

- If $k < n$, the restriction $\mathcal{E}|_F$ is a real phase structure on F of codimension k .
- If $k > 0$, the projection \mathcal{E}^F is a real phase structure on F of codimension $k - 1$.

Proof. • Let σ be a k -simplex of F . The image $\overrightarrow{\pi_F}(T_2^\perp(\sigma))$ is the dual of $T_2(\sigma)$ viewed as a subspace of $T_2(F)$. Thus, the affine space $\mathcal{E}|_F(\sigma) = \pi_F(\mathcal{E}(\sigma))$ is directed by the dual of $T_2(\sigma) \subset T_2(F)$.

It remains to show the parity condition.

Let $s \in \mathcal{Q}^n$. The fiber $\pi_F^{-1}(\pi_F(s))$ consists of two elements:

$$\{s, s + e_F\} = s + T_2^\perp(F).$$

For a k -simplex σ in F , since $T_2^\perp(F) \subset T_2^\perp(\sigma)$, we have $s \in \mathcal{E}(\sigma)$ if and only if $s + e_F \in \mathcal{E}(\sigma)$. Therefore, the condition $\pi_F(s) \in \mathcal{E}|_F(\sigma)$ is equivalent to $s \in \mathcal{E}(\sigma)$. Thus, the parity condition for $\mathcal{E}|_F$ follows directly from the parity condition of \mathcal{E} .

- Let σ be a k -simplex of Δ_n not contained in F . Since Δ_n is unimodular, we have $T(\sigma) + T(F) = \mathbb{Z}^n$, and consequently,

$$T_2^\perp(\sigma \cap F) = T_2^\perp(\sigma) + T_2^\perp(F).$$

Thus, we have the equality $\pi_F^\rightarrow(T_2^\perp(\sigma \cap F)) = \pi_F^\rightarrow(T_2^\perp(\sigma))$. And $\mathcal{E}^F(\sigma \cap F) = \pi_F(\mathcal{E}(\sigma))$ is an affine space directed by the dual of $T_2(\sigma \cap F)$ inside $T_2(F)$.

It remains to show the parity condition. Let $s \in \mathcal{Q}^n$ such that $\pi_F(s) \in \mathcal{E}^F(\sigma \cap F) = \pi_F(\mathcal{E}(\sigma))$. Either $s \in \mathcal{E}(\sigma)$ or $s + e_F \in \mathcal{E}(\sigma)$. But the two possibilities can not both occur simultaneously, as this would imply that e_F , and thus $T_2^\perp(F)$, is contained in the direction $T_2^\perp(\sigma)$ of $\mathcal{E}(\sigma)$ contradicting that σ is not contained in F .

The number of k -simplices σ such that $\pi_F(s) \in \mathcal{E}^F(\sigma \cap F)$ is thus the sum of the number of k -simplices σ such that $s \in \mathcal{E}(\sigma)$ and the number of those such that $s + e_F \in \mathcal{E}(\sigma)$. The parity condition of \mathcal{E}^F for the orthant $\pi_F(s)$ is then a consequence of the parity condition of \mathcal{E} for the orthant s and the orthant $s + e_F$, since the sum of two even numbers is even.

□

The T-manifolds $X_{\mathcal{E}|_F}$ and $X_{\mathcal{E}^F}$ are obtained from $X_{\mathcal{E}}$ in the following way.

The T-manifold $X_{\mathcal{E}|_F}$ is a subcomplex of $X_{\mathcal{E}}$, defined as the intersection $X_{\mathcal{E}} \cap \tilde{F}$. Indeed, we have observed that for a k -simplex σ of F , we have $\pi_F(s) \in \mathcal{E}|_F(\sigma)$ if and only if $s \in \mathcal{E}(\sigma)$. Thus, by identifying $C_{\mathcal{E}}(\pi_F(s)(\sigma)) \subset \tilde{F}$ with $C_{\mathcal{E}}(s(\sigma)) \subset \tilde{\Delta}_n$, we conclude that $X_{\mathcal{E}|_F}$ is the subcomplex of $X_{\mathcal{E}}$ composed of all the cells lying in \tilde{F} .

We now describe the T-manifold $X_{\mathcal{E}^F}$. Denote by v_F the vertex of Δ_n opposite to F . For each point p in Δ distinct from v_F , there is a unique point $\varphi(p)$ of F lying on the line defined by v_F and p . The application φ extends to an application $\tilde{\varphi}: \tilde{\Delta}_n \setminus \{v_F\} \rightarrow \tilde{F}$, where v_F denotes abusively the common image of all the symmetric copies $s(v_F)$ of v_F in the gluing $\tilde{\Delta}$. The image of the barycentric subdivision of $\tilde{\Delta}_n$ under $\tilde{\varphi}$ is the barycentric subdivision of \tilde{F} . More precisely, the image of the barycenter of a face $s(\tau)$ under $\tilde{\varphi}$ is the barycenter of $s(\tau) \cap \tilde{F}$. With this description, we see that the T-manifold associated to the projection $X_{\mathcal{E}^F}$ in \tilde{F} is the image $\varphi(X_{\mathcal{E}})$.

Example 3.5. Consider the real phase structure \mathcal{E}_1 , \mathcal{E}_2 and \mathcal{E}_3 from Examples 2.7, 2.9 and 2.10. Identifying Δ_2 as the facet $[a, b, c]$ of Δ_3 , we have $\mathcal{E}_1 = \mathcal{E}_2|_{\Delta_2}$ and $\mathcal{E}_1 = \mathcal{E}_3^{\Delta_2}$.

3.2. Number of orthants of $\mathcal{E}(\Delta_n)$. In this subsection, we develop the material necessary to prove of Theorem 3.1 on the number of maximal cells.

Lemma 3.6. *Let \mathcal{E} be a k -real phase structure on Δ_n (with $k < n$), and let τ be a $(k+1)$ -simplex of Δ_n . There exists a cyclic order $\sigma_0, \dots, \sigma_{k+1}$ on the k -simplices*

of τ and affine subspaces $\mathcal{B}_i \subset \mathcal{Q}^n$ directed by $T_2^\perp(\tau)$ such that $\mathcal{E}(\sigma_i) = \mathcal{B}_i \cup \mathcal{B}_{i+1}$. Moreover, if F_i is a facet of Δ_n such that $\sigma_i = \tau \cap F_i$, then $\mathcal{B}_{i+1} = \mathcal{B}_i + e_{F_i}$.

Here the indices i are treated modulo $k+2$.

Proof. We prove the first part by induction on $n-k$.

If $n-k=1$, the simplex τ is Δ_n and the k -simplices are the facets F of Δ_n . Recall that spaces $\mathcal{E}(F)$ are lines in \mathcal{Q}^n directed by e_F . Consider all these lines corresponding to facet F of Δ_n . By the parity condition each of the two points of any such line is contained in at least one other line. Suppose the lines corresponding to F_1, \dots, F_m form a cycle, that is, there are points $s_i \in \mathcal{Q}^n$ such that $\mathcal{E}(F_i) = \{s_i, s_{i+1}\}$. Then $\sum_{i=1}^m e_{F_i} = \sum_{i=1}^m \overrightarrow{s_i s_{i+1}} = 0$. However, the only non-trivial relation between the vectors e_F is $\sum_{F \in F_{n-1}(\Delta_n)} e_F = 0$. Thus, the lines form a unique cycle. In other words, there exists a cyclic order F_0, \dots, F_n and points $s_i \in \mathcal{Q}^n$ such that $\mathcal{E}(F_i) = \{s_i, s_{i+1}\}$, which proves the claim in this case.

If $n-k > 1$, consider a facet F of Δ_n containing τ . We apply the heredity property to $\mathcal{E}|_F$ in F . We then obtain a cyclic order $\sigma_0, \dots, \sigma_{k+1}$ and affine subspaces \mathcal{C}_i of $\mathcal{Q}^n/T_2^\perp(F)$ directed by $T_2^\perp(\tau)/T_2^\perp(F)$ such that $\mathcal{E}|_F(\sigma_i) = \mathcal{C}_i \cup \mathcal{C}_{i+1}$. Setting $\mathcal{B}_i = \pi_F^{-1}(\mathcal{C}_i)$, since $e_F \in T_2^\perp(\sigma_i)$, we obtain $\mathcal{E}(\sigma_i) = \pi_F^{-1}(\mathcal{E}|_F(\sigma_i)) = \mathcal{B}_i \cup \mathcal{B}_{i+1}$.

For the second part of the lemma, note that e_{F_i} is in the direction of $\mathcal{E}(\sigma_i)$ but not in the direction of \mathcal{B}_i and \mathcal{B}_{i+1} . Hence, there exist two orthants $s \in \mathcal{B}_i$ and $s' \in \mathcal{B}_{i+1}$ such that $e_{F_i} = s' - s$. Since \mathcal{B}_i and \mathcal{B}_{i+1} are parallel, it follows that $\mathcal{B}_{i+1} = \mathcal{B}_i + e_{F_i}$. \square

Corollary 3.7. *Let \mathcal{E} be a k -real phase structure on Δ_n and let F be a facet of Δ_n . Let σ and σ' be k -faces of a $(k+1)$ -simplex τ of Δ_n .*

For $s \in \mathcal{Q}^n$, if $s \in \mathcal{E}(\sigma)$ and $s + e_F \in \mathcal{E}(\sigma')$, then either $s + e_F \in \mathcal{E}(\sigma)$ or $s \in \mathcal{E}(\sigma')$. In particular, $s \in \mathcal{E}(F)$.

Proof. By Lemma 3.6, we have a cyclic ordering of the k -faces of τ : $\sigma_0, \sigma_1, \dots, \sigma_{k+1}$ and affine subspaces $\mathcal{B}_0, \mathcal{B}_1, \dots, \mathcal{B}_{k+1}$ such that $\mathcal{E}(\sigma_j) = \mathcal{B}_j \cup \mathcal{B}_{j+1}$. Without loss of generality, assume that $s \in \mathcal{B}_0 \subset \mathcal{E}(\sigma_0)$ and $s + e_F \in \mathcal{B}_{i+1} \subset \mathcal{E}(\sigma_i)$.

We partition facets of Δ_n in two categories:

- I_1 : the facets G that contain τ , for which $T_2^\perp(\tau) = \text{span}_{G \in I_1}(e_G)$
- I_2 : the facets F_j , for $0 \leq j \leq k+1$, that intersect τ in the k -simplex σ_j for which $T_2^\perp(\sigma_j) = T_2^\perp(\tau) \oplus T_2^\perp(F_j) = T_2^\perp(\tau) \oplus \{0, e_{F_j}\}$.

Since $\mathcal{B}_{i+1} = \mathcal{B}_i + e_{F_i} = \dots = \mathcal{B}_0 + e_{F_0} + \dots + e_{F_i}$, we have $s' = s + e_{F_0} + \dots + e_{F_i} \in \mathcal{B}_{i+1}$. Hence, the difference $e_{F_0} + \dots + e_{F_i} - e_F$ between s' and $s + e_F$ is in the direction $T_2^\perp(\tau) = \text{span}_{G \in I_1}(e_G)$ of \mathcal{B}_{i+1} . We deduce that

$$e_F = e_{F_0} + e_{F_1} + \dots + e_{F_i} + u$$

where $u \in T_2^\perp(\tau) = \text{span}_{G \in I_1}(e_G)$. This is a linear relation among the e_F 's, for F facet of Δ . However, the only nontrivial relation between the e_F 's is:

$$\sum_{F \in F_{n-1}(\Delta_n)} e_F = 0.$$

Thus, there are three cases:

- $F \in I_1$. In this case, we have both $s + e_F \in \mathcal{E}(\sigma_0)$ and $s \in \mathcal{E}(\sigma_i)$.
- $i = 0$ and $u = 0$. In this case, we have $\sigma_0 \subset F_0 = F$ and $s + e_F \in \mathcal{E}(\sigma_0)$.

- $i = k$ and $u = \sum_{G \in I_1} e_G$. In this case, we have $F = F_{k+1}$ and $s = (s + e_F) - e_F \in \mathcal{E}(\sigma_{k+1}) = \mathcal{E}(\sigma_i)$.

□

Definition 3.8. A path between two k -simplices σ and σ' in Δ_n is a sequence of k -simplices $\sigma^{(0)} = \sigma, \sigma^{(1)}, \dots, \sigma^{(l)} = \sigma'$ such that every consecutive couple $(\sigma^{(i)}, \sigma^{(i+1)})$ share a common $(k-1)$ -simplex (or equivalently, lie on a common $(k+1)$ -simplex).

Lemma 3.9. Let \mathcal{E} be a k -real phase structure on Δ_n . For any $\sigma, \sigma' \in F_k(\Delta_n)$ and $s \in \mathcal{Q}^n$, if $s \in \mathcal{E}(\sigma) \cap \mathcal{E}(\sigma')$, then there exist $\sigma^{(0)}, \sigma^{(1)}, \dots, \sigma^{(l)}$ a path between σ and σ' such that $s \in \mathcal{E}(\sigma^{(i)})$ for all i between 0 and l .

Proof. For $k = n$, necessarily $\sigma = \Delta_n = \sigma'$ and the result is trivial.

For $k = 0$, a vertex v satisfies $T_2^\perp(v) = (\mathbb{F}_2^n)^\vee$, so $\mathcal{E}(v) = \mathcal{Q}^n$ and any path works.

Otherwise, we proceed by induction on n : We may suppose σ and σ' share at least one vertex.

Indeed, if they do not, select a vertex v of σ' and let τ be the $(k+1)$ -simplex containing σ and having v as one of its vertices.

The parity condition of \mathcal{E} on τ and s ensures that there exists another k -simplex $\sigma'' \neq \sigma$ inside τ such $s \in \mathcal{E}(\sigma'')$.

Now σ'' and σ' share the vertices v . So up to replacing σ' by σ'' , we suppose σ and σ' share a vertex.

Let F be the facet dual to a shared vertex of σ and σ' . Consider the projection \mathcal{E}^F . We have

$$\pi_F(s) \in \mathcal{E}^F(\sigma \cap F) \cap \mathcal{E}^F(\sigma' \cap F).$$

Thus, by induction hypothesis, there exists a path $\sigma^{(0)} = \sigma, \dots, \sigma^{(l)} = \sigma'$ such that $\pi_F(s) \in \mathcal{E}^F(\sigma^{(i)} \cap F)$.

By definition of \mathcal{E}^F , it implies that, for each i , either s or $s + e_F$ is in $\mathcal{E}(\sigma^{(i)})$.

Let m (resp. M) the minimal (resp. maximal) index such $s \notin \mathcal{E}(\sigma^{(i)})$.

Since $s \in \mathcal{E}(\sigma^{(m-1)})$ and $s + e_F \in \mathcal{E}(\sigma^{(m)})$ and since $\sigma^{(m-1)}$ and $\sigma^{(m)}$ lie in a common $(k+1)$ -face, it follows that $s + e_F \in \mathcal{E}(\sigma^{(m-1)})$ by Corollary 3.7.

Consequently, the simplex $\sigma^{(m-1)}$ must be contained in F . Similarly, the simplex $\sigma^{(M+1)}$ must also be contained in F .

Consider the restriction $\mathcal{E}|_F$.

We have $\pi_F(s) \in \mathcal{E}|_F(\sigma^{(m-1)}) \cap \mathcal{E}|_F(\sigma^{(M+1)})$.

By induction hypothesis, there exists a path $\tilde{\sigma}^{(1)}, \dots, \tilde{\sigma}^{(L)}$ between $\sigma^{(m-1)}$ and $\sigma^{(M+1)}$ in F such that $\pi_F(s) = \mathcal{E}|_F(\tilde{\sigma}^{(i)})$.

Combining the paths, we obtain the desired path:

$$\sigma^{(0)}, \sigma^{(1)}, \dots, \sigma^{(m-1)} = \tilde{\sigma}^{(1)}, \dots, \tilde{\sigma}^{(L)} = \sigma^{(M+1)}, \dots, \sigma^{(l)}$$

This completes the proof. □

Proposition 3.10. Let Δ_n be a n -dimensional lattice simplex and \mathcal{E} a k -real phase structure on Δ_n . Then

$$|\mathcal{E}(\Delta_n)| = \sum_{i=k}^n \binom{n}{i}.$$

Proof. For $k = 0$, we have $\mathcal{E}(v) = \mathcal{Q}^n$ for any vertex, so

$$|\mathcal{E}(\Delta_n)| = |\mathcal{Q}^n| = 2^n = \sum_{i=0}^n \binom{n}{i}.$$

For $k = n$, the vector space $T_2^\perp(\Delta_n)$ is trivial, hence $\mathcal{E}(\Delta_n)$ consists of a single point. Therefore,

$$|\mathcal{E}(\Delta_n)| = 1 = \binom{n}{n}.$$

Otherwise, we proceed by induction on the dimension n of Δ_n . The base case $n = 0$ is already included in the case $k = 0$ above, so we may assume $n > k > 0$

Fix a facet F of Δ_n . We divide each $s \in \mathcal{E}(\Delta_n)$ in two categories depending on their relationship with F . An orthant s belongs to the first category if $s + e_F \in \mathcal{E}(\Delta_n)$; otherwise, s belongs to the second category.

In the first category, we have $s \in \mathcal{E}(F)$. Indeed, suppose $s \in \mathcal{E}(\sigma)$ and $s + e_F \in \mathcal{E}(\sigma')$ for some k -simplices σ, σ' of Δ_n . If either σ or σ' is in F , we are done. Otherwise, consider $\pi_F(s) \in \mathcal{E}^F(\sigma \cap F) \cap \mathcal{E}^F(\sigma' \cap F)$. By Lemma 3.9, we have a path $\sigma^{(1)}, \dots, \sigma^{(l)}$ such that $\pi_F(s) \in \mathcal{E}^F(\sigma^{(i)} \cap F)$ for each i . Since $s \in \mathcal{E}(\sigma)$ and $s + e_F \in \mathcal{E}(\sigma')$, we have an index i such that $s \in \mathcal{E}(\sigma^{(i)})$ and $s + e_F \in \mathcal{E}(\sigma^{(i+1)})$. And the Corollary 3.7 implies that $s \in \mathcal{E}(F)$.

In the second category, we have $s \notin \mathcal{E}(F)$. So $\pi_F(s) \notin \mathcal{E}_{|F}(F)$ but $\pi_F(s) \in \mathcal{E}^F(F)$.

Denote a the number of pair $\{s, s + e_F\}$ of the first category and b the number of element s of the second category. The previous discussion shows that $|\mathcal{E}(\Delta_n)| = 2a + b$, $|\mathcal{E}^F(F)| = a + b$ and $|\mathcal{E}_{|F}(F)| = a$. Hence, $|\mathcal{E}(\Delta_n)| = |\mathcal{E}_{|F}(F)| + |\mathcal{E}^F(F)|$. Now we can apply the recursion hypothesis on \mathcal{E}^F and $\mathcal{E}_{|F}$:

$$|\mathcal{E}_{|F}(F)| = \sum_{i=k}^{n-1} \binom{n-1}{i} \text{ and } |\mathcal{E}^F(F)| = \sum_{i=k-1}^{n-1} \binom{n-1}{i}.$$

Now using Pascal's formula:

$$\begin{aligned} |\mathcal{E}(\Delta_n)| &= |\mathcal{E}_{|F}(F)| + |\mathcal{E}^F(F)| \\ &= \sum_{i=k}^{n-1} \binom{n-1}{i} + \sum_{i=k-1}^{n-1} \binom{n-1}{i} \\ &= \sum_{i=k}^{n-1} \left[\binom{n-1}{i} + \binom{n-1}{i-1} \right] + \binom{n-1}{n-1} \\ &= \sum_{i=k}^{n-1} \binom{n}{i} + \binom{n}{n} \\ &= \sum_{i=k}^n \binom{n}{i} \end{aligned}$$

□

Proof of Theorem 3.1. For each n -simplex σ of Γ , the simplex $s(\sigma)$ contains a maximal cell of $X_{\mathcal{E}}$ if and only if $s \in \mathcal{E}(\sigma)$. Thus, by Theorem 3.10, each n -simplex of γ contributes to $\sum_{i=k}^n \binom{n}{i}$ maximal cells of $X_{\mathcal{E}}$. Since Γ is unimodular, it contains a number of n -simplices equal to $\text{Vol}(\Delta)$.

Hence, the total number of maximal cells in the canonical decomposition of $X_{\mathcal{E}}$ is $\sum_{i=k}^n \binom{n}{i} \text{Vol}(\Delta)$. □

If $s \in \mathcal{E}(\Delta_n)$, s is called a non-empty orthant.

3.3. Number of simplicial orthants. In this subsection, we detail the necessary material to obtain the proof of the Theorem 3.2 on the number of simplicial cells.

Lemma 3.11. *Let $s \in \mathcal{E}(\Delta_n)$. Then one has*

$$|\{\sigma \in F_k(\Delta_n) | s \in \mathcal{E}(\sigma)\}| \geq n - k + 1.$$

In case of equality, the simplices of $\{\sigma \in F_k(\Delta_n) | s \in \mathcal{E}(\sigma)\}$ are all adjacent but no three of them can lie in a common $(k+1)$ -simplex.

Proof. Since $s \in \mathcal{E}(\Delta_n)$, there exists a k -simplex σ such that $s \in \mathcal{E}(\sigma)$. Now consider any $(k+1)$ -simplex τ that contains σ . The parity condition ensures that there exists another k -simplex σ' such that $s \in \mathcal{E}(\sigma')$. Each choice of τ corresponds to a choice of a vertex from Δ_n that is not already in σ . Since Δ_n has $n+1$ vertices, and σ has $k+1$ vertices, there are $n-k$ possible ways to choose τ . Each such choice of τ yields a distinct k -simplex, since the intersection of two distinct $(k+1)$ -simplices can not contain two distinct k -simplices. Therefore, starting from the initial k -simplex σ , we can find $n-k$ additional k -simplices, leading to a total of at least $n-k+1$ such simplices. \square

A non-empty orthant s for which this inequality holds as equality is called **simplicial**. The name come from the fact that for $s \in \mathcal{E}(\Delta_n)$, the $n-k$ -cell $C_{\mathcal{E}}(s(\Delta_n))$ contains a number of 0-cells corresponding to $|\{\sigma \in F_k(\Delta_n) | s \in \mathcal{E}(\sigma)\}|$. Thus, if $s \in \mathcal{E}(\Delta_n)$ is simplicial, the cell $C_{\mathcal{E}}(s(\Delta_n))$ is a simplicial cell in the canonical cell decomposition of $X_{\mathcal{E}}$.

Example 3.12.

- If $k = n$, the polytope Δ_n has only one k -simplex (which is Δ_n itself), thus the unique non-empty orthant of \mathcal{E} is simplicial.
- If $k = 0$, the k -simplices are the vertices of Δ_n and $\mathcal{E}(v) = \mathcal{Q}^n$. Thus, all orthants are simplicial.
- If $k = n-1$, all non-empty orthants are simplicial. Indeed, $C_{\mathcal{E}}(s(\Delta_n))$ is a cell of dimension 1 and thus contains exactly two 0-cells.
- In the Example 2.9, the orthant $(-, +, -)$ is empty. The four orthants $(-, +, +)$, $(+, -, +)$, $(+, +, -)$ and $(-, -, -)$, represented in green by in Figure 2, are simplicial. The three other orthants $(+, +, +)$, $(-, -, +)$ and $(+, -, -)$, represented in red, are non-simplicial.

Lemma 3.13. *Suppose $k \leq n-1$. Let $s \in \mathcal{E}(\Delta_n)$ be a simplicial orthant. Then there exists a $(k-1)$ -simplex γ such that for all k -simplex σ ,*

$$s \in \mathcal{E}(\sigma) \iff \gamma \subset \sigma.$$

Proof. First, notice that by the Lemma 3.11, if s is simplicial then all k -simplices σ such that $s \in \mathcal{E}(\sigma)$ are adjacent to each other, and no three of them can lie in a same $(k+1)$ -simplex.

Fix three of these k -simplices: $\sigma^{(0)}$, $\sigma^{(1)}$ and $\sigma^{(2)}$. We only need to show that $\gamma^{(1)} = \sigma^{(1)} \cap \sigma^{(0)}$ and $\gamma^{(2)} = \sigma^{(2)} \cap \sigma^{(0)}$ are the same $(k-1)$ -simplex.

Since $\sigma^{(1)}$ and $\sigma^{(2)}$ are adjacent, they are both in a $(k+1)$ -simplex τ . The simplex $\tau \cap \sigma^{(0)}$ is contained in the k -simplex $\sigma^{(0)}$, and it contains the $(k-1)$ -simplex $\sigma^{(1)} \cap \sigma^{(0)} = \gamma^{(1)}$.

Thus, we have two possibilities: $\tau \cap \sigma^{(0)} = \sigma^{(0)}$ or $\tau \cap \sigma^{(0)} = \gamma^{(1)}$.

If we are in the first case, then $\sigma^{(0)}$, $\sigma^{(1)}$ and $\sigma^{(2)}$ are both contained in the $(k+1)$ -simplex τ , which contradicts that s is simplicial. Thus, we must be in the second case: $\tau \cap \sigma^{(0)} = \gamma^{(1)}$.

Since by construction $\sigma^{(2)} \subset \tau$, we also have $\gamma^{(2)} = \sigma^{(2)} \cap \sigma^{(0)} \subset \tau \cap \sigma^{(0)} = \gamma^{(1)}$. By equality of the dimensions, we can conclude that $\gamma^{(1)} = \gamma^{(2)}$. \square

Proposition 3.14. *The number $S_{n,k}$ of simplicial orthants in \mathcal{E} is at most $\frac{2}{k+1} \binom{n+1}{k}$.*

Proof. We proceed by induction on n . If $n = k$, there is only one orthant which is always simplicial. Thus, we have $S_{n,n} = 1 < \frac{2}{n+1} \binom{n+1}{n}$.

If $n = k + 1$, the bound is also trivial:

$$S_{n,n-1} = |\mathcal{E}(\Delta)| = n + 1 = \frac{2}{n} \binom{n+1}{n-1}$$

Suppose $k < n - 1$. Let s be simplicial orthant and γ the $(k-1)$ -simplex described in Lemma 3.13. For each face F of Δ_n containing γ , observe that $\pi_F(s)$ is a simplicial orthant of $\mathcal{E}|_F$. Indeed, for every k -simplex σ of F , we have the equivalence

$$\pi_F(s) \in \mathcal{E}|_F(\sigma) \iff s \in \mathcal{E}(\sigma).$$

Among all k -simplices of Δ_n containing γ , exactly one does not lie in F , therefore $|\{\sigma \in F_k(F) | s \in \mathcal{E}|_F(\sigma)\}| = |\{\sigma \in F_k(\Delta_n) | s \in \mathcal{E}(\sigma)\}| - 1 = n - k$. Hence, $\pi_F(s)$ is indeed simplicial in $\mathcal{E}|_F$.

Consequently, a simplicial orthant s in \mathcal{E} gives a simplicial orthant in $\mathcal{E}|_F$ for each of the $n+1-k$ facets F containing γ .

By a double counting of the pairs (s, F) where s is a simplicial orthant of \mathcal{E} such that $\pi_F(s)$ is a simplicial orthant of $\mathcal{E}|_F$, we obtain $(n+1-k)S_{n,k} \leq (n+1)S_{n-1,k}$. By induction, we have $S_{n,k} \leq \frac{n+1}{n+1-k} \frac{2}{k+1} \binom{n}{k} = \frac{2}{k+1} \binom{n+1}{k}$. \square

Proof of Theorem 3.2. For each n -simplex σ of Γ , the simplex $s(\sigma)$ contains a simplicial cell of $X_{\mathcal{E}}$ if and only if s is a simplicial orthant of $\mathcal{E}(\sigma)$. Thus, by Theorem 3.14, each n -simplex of γ contributes to at most $\frac{2}{k+1} \binom{n+1}{k}$ simplicial orthants. Since Γ is unimodular, it contains a number of n -simplices equal to $\text{Vol}(\Delta)$.

Hence, the total number of simplicial cells in the canonical decomposition of $X_{\mathcal{E}}$ is at $\frac{2}{k+1} \binom{n+1}{k} \text{Vol}(\Delta)$. \square

4. BOUNDS ON THE NUMBER OF CONNECTED COMPONENTS OF T-MANIFOLDS

4.1. Maximal T-curves. In this section, we consider a lattice polytope Δ in \mathbb{R}^n equipped with a unimodular triangulation Γ and a real phase structure \mathcal{E} on the $(n-1)$ -skeleton of Γ . In this context, the T-manifold $X_{\mathcal{E}}$ is a curve. The canonical cell decomposition of $X_{\mathcal{E}}$ consists of 0-cells and 1-cells:

- The 0-cells $C_{\mathcal{E}}(s(\sigma))$ correspond to the $(n-1)$ -simplices σ of $F_{n-1}(\Gamma)$ with $s \in \mathcal{E}(\sigma)$.
- The 1-cells $C_{\mathcal{E}}(s(\tau))$ correspond to the n -simplices τ of $F_n(\Gamma)$ with $s \in \mathcal{E}(\tau)$

We will study the number of connected components $b_0(X_{\mathcal{E}})$ of the T-curve $X_{\mathcal{E}}$.

Definition 4.1. The dual graph G_{Γ} of the subdivision Γ is defined as follows:

The set of vertices of G_{Γ} consists of v_{τ} for each n -simplex $\tau \in F_n(\Gamma)$ and u_{σ} for each $(n-1)$ -dimensional simplex $\sigma \in F_{n-1}(\Gamma)$ that lies on the boundary of Δ .

The set of edges of G_{Γ} consist of e_{σ} for each $(n-1)$ -simplex σ of $F_{n-1}(\Gamma)$.

- If σ is an interior $(n-1)$ -simplex, the vertices adjacent to the edge e_{σ} correspond to the two adjacent n -simplices: v_{τ} and $v_{\tau'}$.

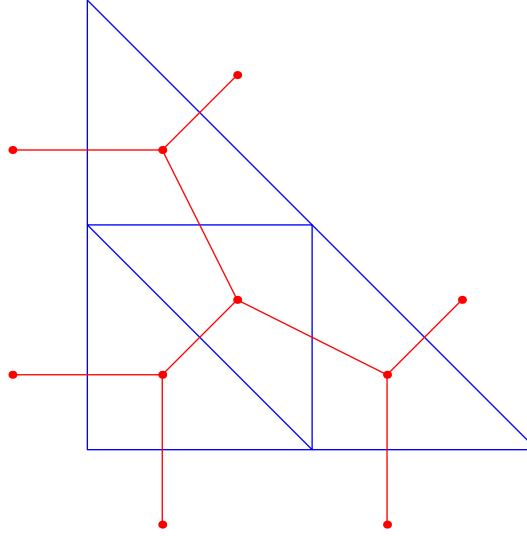


FIGURE 5. In blue, a subdivision and, in red, its dual graph.

- If σ is a boundary $(n-1)$ -simplex, the vertices adjacent to the edge e_σ correspond to the vertex v_τ of the unique adjacent n -simplex and the vertex u_σ .

Remark 4.2. This kind of graph appears in tropical geometry. To a tropical hypersurface Σ in \mathbb{R}^n is associated a dual polytope known as the Newton polytope. The tropical hypersurface also induces a convex triangulation Γ of the Newton polytope. In this case, the dual graph G_Γ is the graph of the 1-skeleton of Σ where the unbounded rays of Σ have been compactified by vertices.

For a triangulation Γ of $\Delta \subset \mathbb{R}^n$, the vertices v_τ (corresponding to the n -simplices) of G_Γ have degree $n+1$, while the vertices u_σ (corresponding to the $(n-1)$ -simplices on the boundary) have degree 1.

For a smooth real algebraic compact curve, by the Harnack-Klein theorem [Kle76], the number of connected components of the real part is bounded by the genus of the complex part plus one. As observed by Haas in [Haa97], this inequality has a combinatorial analogue for T-curves in toric surfaces. The following proposition generalizes this inequality to higher ambient dimensions and gives a condition for the equality to hold. In this setting, the role of the genus of the complex part is played by the first Betti number $b_1(G_\Gamma)$ of the graph homology.

Recall that a graph G is said planar if it can be embedded (with no crossing edges) in \mathbb{R}^2 or equivalently in the sphere S^2 .

Proposition 4.3. *Let (Δ, Γ) be a triangulated polytope of dimension n and \mathcal{E} be a real phase structure on the $(n-1)$ -skeleton of Γ . We have the following bound:*

$$(2) \quad b_0(X_{\mathcal{E}}) \leq b_1(G_\Gamma) + 1$$

Moreover in the case of equality, the graph G_Γ is planar.

Proof. First, observe that to each 0-cell $C_{\mathcal{E}}(s(\sigma))$, with $\sigma \in F_{n-1}(\Gamma)$ and $s \in \mathcal{E}(\sigma)$, we can associate the edge e_σ in G_Γ . Conversely, since for $\sigma \in F_{n-1}(\Gamma)$ the affine

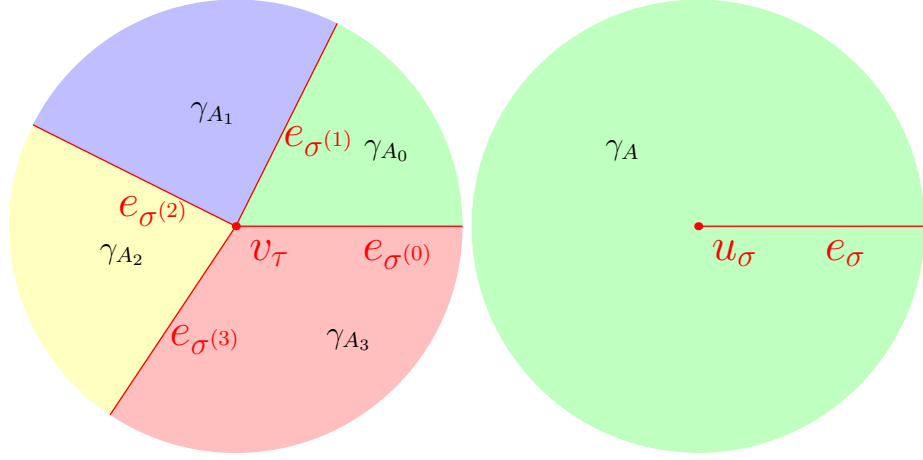


FIGURE 6. An illustration of the gluing defining the surface S in the proof of proposition 4.3

space $\mathcal{E}(\sigma)$ is one dimensional, it consists of exactly two orthants $\{s, s'\}$. Thus, the edge e_σ of G_Γ is associated to two 0-cells $C_{\mathcal{E}}(s(\sigma))$ and $C_{\mathcal{E}}(s'(\sigma))$ in $X_{\mathcal{E}}$. If the two $(n-1)$ -simplices $s(\sigma)$ and $s(\sigma')$ are identified in Δ (which happen exactly when σ is a boundary simplex), $C_{\mathcal{E}}(s(\sigma))$ and $C_{\mathcal{E}}(s'(\sigma))$ are in fact the same cell but, in this case, we count the cell twice.

For each connected component A of $X_{\mathcal{E}}$, the succession of 0-cells of A defines a succession of edges in G_Γ , which in turn forms a cycle γ_A in G_Γ (potentially with repeating edges).

For each cycle γ_A , attach a disk by gluing their boundary along γ_A . This defines a two-dimensional compact CW-complex S , which we claim is a topological surface. Indeed, since each edge correspond to two 0-cells, it appears either in two cycles γ_A or twice in a single cycle. This implies that the interior of an edge locally looks like the gluing of two half-planes. Furthermore, for a n -simplex τ , by Lemma 3.6, we have a cyclic order $\sigma_0, \sigma_1, \dots, \sigma_n$ of the $(n-1)$ -simplices in τ and orthant $s_i \in \mathcal{Q}^n$ such that $\mathcal{E}(\sigma^{(i)}) = \{s_i, s_{i+1}\}$ taking the value of i modulo $n+1$. Thus, there are cycles γ_{A_i} containing successively $e_{\sigma^{(i)}}$ and $e_{\sigma^{(i+1)}}$. Hence, the neighborhood of v_τ in S is homeomorphic to \mathbb{R}^2 (see Figure 6). Finally, for a $(n-1)$ -simplex σ on the boundary with $\mathcal{E}(\sigma) = \{s_1, s_2\}$, the 1-cells $C_{\mathcal{E}}(s_1(\sigma))$ and $C_{\mathcal{E}}(s_2(\sigma))$ are adjacent and a fortiori belong to the same connected component A . Thus, the neighborhood of u_σ is also homeomorphic to \mathbb{R}^2 . Therefore, S is indeed a closed connected surface.

Let's compute its Euler characteristic $\chi(S)$: the complex S is composed of V vertices, E edges and $F = b_0(X_{\mathcal{E}})$ faces, so $\chi(S) = V - E + F$. But looking at Euler characteristic of G_Γ , we have $V - E = \chi(G_\Gamma) = b_0(G_\Gamma) - b_1(G_\Gamma) = 1 - b_1(G_\Gamma)$ since G_Γ is connected. So $\chi(S) = b_0(X_{\mathcal{E}}) + 1 - b_1(G_\Gamma)$. But for a connected compact surface, the Euler characteristic is less than 2 with the equality case only for the sphere. It follows that $b_0(X_{\mathcal{E}}) + 1 - b_1(G_\Gamma) \leq 2$ or $b_0(X_{\mathcal{E}}) \leq b_1(G_\Gamma) + 1$ with equality only if S is a sphere. Furthermore, in this case, the inclusion $G_\Gamma \subset S$ gives a planar embedding of G_Γ . \square

Remark 4.4. When Δ is smooth, it follows from the Theorem 1.4 of [BLdMR24] that the inequality 4.3 correspond to the case $k = n - 1$ and $p = 0$ of the inequality 1. More precisely, $h^{0,1}(Y_\Delta^{n-1}) = b_1(G_\Gamma)$ and $h^{0,0}(Y_\Delta^{n-1}) = 1$. In this light, we say that the T-curve $X_\mathcal{E}$ is maximal when $b_0(X_\mathcal{E}) = b_1(G_\Gamma) + 1$.

The proof above provides a direct and elementary justification of this special case, which additionally gives a condition on the equality case.

When the dual graph is trivalent, a study of maximal T-curve can be found in [BBR17].

By Kuratowski's theorem [Tho81], a graph is planar if and only if it contains no subgraph that is a subdivision of the complete graph K_5 or the complete bipartite graph $K_{3,3}$.

Proposition 4.5. *Let Δ be an n -dimensional lattice polytope with a unimodular triangulation Γ . If Δ has an interior lattice point p , then G_Γ contains a subgraph that is a subdivision of the complete graph on $n + 1$ vertices K_{n+1} .*

Proof. Since Γ is unimodular, the point p is the vertex of an n -dimensional simplex σ of Γ . Each facet of σ containing p is an interior simplex of Δ and thus is contained in another maximal simplex. Let $\sigma_1, \dots, \sigma_n$ denote these maximal simplices. Consider the vertices v, v_1, \dots, v_n of the graph G_Γ corresponding to the n -simplex $\sigma, \sigma_1, \dots, \sigma_n$.

We claim that every pair of these $n + 1$ vertices can be connected by a path in G_Γ such that these paths are disjoint (excepted for their endpoints). Together, they form a subdivision of K_{n+1} .

The path between v and v_i is just the edge $v - v_i$, since σ and σ_i share a facet.

For v_i and v_j , consider the intersection $\sigma \cap \sigma_i \cap \sigma_j$: this is a $(n - 2)$ -simplex $\gamma_{i,j}$ containing p . As $\gamma_{i,j}$ is an interior $(n - 2)$ -simplex, the vertices of G_Γ corresponding to simplex containing $\gamma_{i,j}$ form a cycle. This cycle includes the path $v_i - v - v_j$ and the complementary part of the cycle provides the desired path between v_i and v_j .

We now show that the paths are disjoint. It is direct for the path $v - v_i$. Suppose w is a vertex contained both in the path between v_i and v_j and in the path between $v_{i'}$ and $v_{j'}$, with $\{i, j\} \neq \{i', j'\}$. The vertices w of G_Γ must correspond to an n -simplex of Γ containing both $\gamma_{i,j}$ and $\gamma_{i',j'}$. Since the simplex containing $\gamma_{i,j}$ and $\gamma_{i',j'}$ is a facet of σ containing p or σ itself, the vertex w can only be v, v_1, \dots, v_{n-1} or v_n . Hence, all our paths only meet at their endpoints. \square

We immediately deduce the following restriction on the existence of maximal T-curves.

Corollary 4.6. *Let Δ be a lattice polytope of dimension $n > 3$ with an interior lattice point. For any real phase structure \mathcal{E} on the $(n - 1)$ -skeleton of a triangulation of Δ , the T-curve $X_\mathcal{E}$ is not maximal.*

Proof. By proposition 4.5, the graph G_Γ contains a subdivision of K_{n+1} with $n \geq 4$. Since K_m is not planar for $m \geq 5$, the graph G_Γ is not planar. Hence, by proposition 4.3, the T-curve $X_\mathcal{E}$ is not maximal. \square

Ehrhart theory of lattice polytope provides powerful tools to study the existence of interior points. See [BR15] for details on this topic.

Definition 4.7. The codegree of a lattice polytope Δ is the minimal integer k such that $k\Delta$ has no interior lattice point.

The codegree can be computed from the f -vector of a unimodular triangulation Γ . But we restrict ourselves to this simple bound on the codegree.

Proposition 4.8. *The codegree of a lattice polytope Δ of dimension n is less than $n + 1$ with equality if and only if Δ is a unimodular simplex.*

Corollary 4.9. *Let Δ be a lattice polytope of dimension $n > 3$ and $d \geq n + 1$. For any real phase structure \mathcal{E} on the $(n - 1)$ -skeleton of a triangulation of $d\Delta$, the T-curve $X_{\mathcal{E}}$ is not maximal. If Δ is not a unimodular simplex, we can even take $d = n$.*

Proof. By proposition 4.8, the hypothesis of Corollary 4.6 is satisfied hence also its conclusion. \square

For $n = 2$, maximal T-curve can be constructed for any polygon[Haa97].

For $n = 3$, the assumption that G_{Γ} is planar is already pretty restrictive. However, we present in Section 6 a maximal T-curve in $d\Delta_3$, for any $d \geq 1$.

4.2. Bounds on the number of connected components of T-curves. In the previous subsection, we have shown there are no maximal T-curves in ambient dimension $n > 3$ when the polytope contains interior points. But can we still have T-curve approaching maximality? Is the bound of proposition 4.3 still, at least asymptotically, optimal?

Here, we construct a new bound on the number of connected component of T-curves by enumerating the number of 1-cells of a T-curve. It turns out this bound is stronger than the one from 4.3 for dilation of polytope in high dimension.

Theorem 4.10. *Let Δ be a lattice polytope of dimension n . For any T-curve $X_{\mathcal{E}}$ with Newton polytope Δ , one has*

$$(3) \quad b_0(X_{\mathcal{E}}) \leq \frac{n+1}{3} \text{Vol}(\Delta)$$

Proof. By Theorem 3.1, the number of 1-cells in the canonical cell decomposition of $X_{\mathcal{E}}$ is $(n + 1) \text{Vol}(\Delta)$.

However, because two maximal simplices share at most one facet, a connected component of $X_{\mathcal{E}}$ must pass through at least three different maximal simplices of $\tilde{\Delta}$. Thus, each of the $b_0(X_{\mathcal{E}})$ connected components of $X_{\mathcal{E}}$ is made of at least three 1-cells. Hence, the inequality:

$$3b_0(X_{\mathcal{E}}) \leq (n + 1) \text{Vol}(\Delta)$$

\square

To compare the bounds 2 and 3, we need to relate the homology of G_{Γ} with the volume of Δ .

By a slight abuse of notation, we denote $\text{Vol}(\partial\Delta)$ the sum, over all facet F of Δ , of the lattice volume $\text{Vol}(F)$, where F is considered as a full dimensional polytope in their tangent lattice $T(F)$. For example, we have $\text{Vol}(\partial\Delta_n) = n + 1$.

Lemma 4.11. *Let Δ be an n -dimensional polytope with $\alpha = \text{Vol}(\Delta)$ and $\beta = \text{Vol}(\partial\Delta)$. Then for any unimodular triangulation Γ , the first Betti number of G_{Γ} is $b_1(G_{\Gamma}) = \frac{(n-1)\alpha-\beta}{2} + 1$.*

Proof. The unimodular triangulation Γ contains α maximal simplices and β $(n-1)$ -simplices on the boundary of Δ . Thus, G_Γ is made of α vertices of degree $n+1$ and β vertices of degree 1. By the handshaking lemma, the number of edges of G_Γ is thus $\frac{(n+1)\alpha+\beta}{2}$. Computing Euler characteristic leads to: $b_0(G_\Gamma) - b_1(G_\Gamma) = (\alpha+\beta) - \frac{(n+1)\alpha+\beta}{2}$. Given that G_Γ is connected, we obtain $b_1(G_\Gamma) = \frac{(n-1)\alpha-\beta}{2} + 1$. \square

Considering dilation of Δ , we have the following volume relationships:

$$\text{Vol}(d\Delta) = d^n \text{Vol}(\Delta) = d^n \alpha \text{ and } \text{Vol}(\partial(d\Delta)) = d^{n-1} \text{Vol}(\partial\Delta) = d^{n-1} \beta.$$

Thus, for a T-curve X_d with Newton polytope $d\Delta$, the proposition 4.3 gives us

$$(4) \quad b_0(X_d) \leq \frac{(n-1)d^n \alpha - d^{n-1} \beta}{2} + 2$$

with equality for maximal curves. Meanwhile, the bound (3) is $b_0(X_d) \leq \frac{(n+1)d^n \alpha}{3}$. For $n > 5$, the latter bound is asymptotically better as d tends to infinity.

Proposition 4.12. *Let Δ be a lattice polytope of dimension $n > 5$ with volume $\alpha = \text{Vol}(\Delta)$ and boundary volume $\beta = \text{Vol}(\partial\Delta)$. For a T-curve X_d in $d\Delta$, the bound (3) is stricter than the bound (2), for d large enough. More precisely,*

$$b_0(X_d) \leq \frac{n+1}{3} d^n \alpha < b_1(G_\Gamma) + 1$$

for any $d > 2$ such that $(n-5)\alpha d \geq 3\beta$.

Proof. By equation (5), we have $b_1(G_\Gamma) + 1 = \frac{(n-1)d^n \alpha - d^{n-1} \beta}{2} + 2$. Thus, the inequality to check is

$$\frac{n+1}{3} d^n \alpha < \frac{(n-1)d^n \alpha - d^{n-1} \beta}{2} + 2$$

which is equivalent to

$$(5) \quad 3\beta < (n-5)d\alpha + 12d^{1-n}.$$

Since we supposed $n > 5$ and $d > 1$, we have $12d^{1-n} < \frac{3}{8} < 1$. Hence, (5) is equivalent to $3\beta \leq (n-5)d\alpha - 1$ since the quantities are integers. \square

Corollary 4.13. *Let Δ be a lattice polytope of dimension $n > 5$. There is no asymptotically maximal family $(X_d)_{d \geq 1}$ of T-curve with Newton polytope Δ .*

4.3. Bounds on the number of connected components of T-surfaces. We now use a slight variation of the method used for T-curves to derive new bounds on the number of connected components of maximal T-surfaces. In this subsection \mathcal{E} is $(n-2)$ -real phase structure.

Theorem 4.14. *Let Δ be an n -dimensional lattice polytope and let $X_\mathcal{E}$ be a T-surface in Δ . Then,*

$$b_0(X_\mathcal{E}) \leq \frac{7n^2 + 5n + 12}{60} \text{Vol}(\Delta).$$

Proof. By Theorem 3.1, $X_\mathcal{E}$ consists of $f = [\frac{n(n-1)}{2} + n + 1] \text{Vol}(\Delta)$ faces, and by Theorem 3.2, at most $t = \frac{2}{n-1} \binom{n+1}{n-2} \text{Vol}(\Delta) = \frac{n(n-1)}{3} \text{Vol}(\Delta)$ of these are triangles.

Let p_m be the number of connected components of $X_\mathcal{E}$ with exactly m 2-faces. The total number of connected components is $b_0(X_\mathcal{E}) = \sum_m p_m$. Since a face of $X_\mathcal{E}$ has at least three adjacent faces, a connected component of $X_\mathcal{E}$ is made of at least 4 faces, thus $p_i = 0$ for $i < 4$. In a component with exactly four faces

(that is contributing to p_4), all these faces must be triangles. Thus, we obtain $4p_4 \leq t$. The total number of faces can be estimated as follows: $f = \sum_{m \geq 0} mp_m = 4p_4 + \sum_{m \geq 5} mp_m \geq 4p_4 + \sum_{m \geq 5} 5p_m = 5b_0(X_{\mathcal{E}}) - p_4$. Combining these inequalities yields

$$b_0(X_{\mathcal{E}}) \leq \frac{4f + t}{20} = \frac{7n^2 + 5n + 12}{60} \text{Vol}(\Delta).$$

□

To compare this bound to the maximality criterion (1), we need to evaluate the Hodge numbers $h^{0,q}(Y_{\Delta}^k)$. Khovanskii [Kho78] computed these numbers for any generic complete intersection in toric variety:

$$h^{0,q}(Y_{\Delta}^k) = \begin{cases} 1 & \text{if } q = 0 \\ \sum_{l=1}^k \binom{k}{l} (-1)^{k-l} |\text{int}(l\Delta) \cap \mathbb{Z}^n| & \text{if } q = n - k \\ 0 & \text{otherwise} \end{cases}$$

This expression can be rewritten in terms of the Ehrhart polynomial using the reciprocity law:

$$h^{0,n-k}(Y_{\Delta}^k) = \sum_{l=1}^k \binom{k}{l} (-1)^{n+k-l} P_{\Delta}(-l),$$

where P_{Δ} is the Ehrhart polynomial of Δ , defined by $P_{\Delta}(t) = |t\Delta \cap \mathbb{Z}^n|$, for t a positive integer.

Lemma 4.15. *The sum $\sum_{q=0}^{n-k} h^{0,q}(Y_{d\Delta}^k)$ is a rational polynomial in d whose leading term is*

$$\frac{k!}{n!} \left\{ \begin{matrix} n \\ k \end{matrix} \right\} \text{Vol}(\Delta) d^n,$$

where $\left\{ \begin{matrix} n \\ k \end{matrix} \right\}$ denotes the Stirling number of the second kind.

Proof. Since $P_{d\Delta}(x) = P_{\Delta}(dx)$, we have

$$\sum_{q=0}^{n-k} h^{0,q}(Y_{d\Delta}^k) = 1 + \sum_{l=1}^k \binom{k}{l} (-1)^{k-l} P_{\Delta}(-dl).$$

As P_{Δ} is a rational polynomial of degree $n = \dim \Delta$ with leading coefficient $\frac{\text{Vol}(\Delta)}{n!}$, the sum of Hodge numbers is a polynomial in d with leading term

$$\sum_{l=1}^k (-1)^{n+k-l} \binom{k}{l} \frac{\text{Vol}(\Delta)}{n!} (-ld)^n.$$

The formula for Stirling numbers of the second kind $\left\{ \begin{matrix} n \\ k \end{matrix} \right\} = \frac{1}{k!} \sum_{l=0}^k (-1)^{k-l} \binom{k}{l} l^n$ gives the desired leading term $\frac{k!}{n!} \left\{ \begin{matrix} n \\ k \end{matrix} \right\} \text{Vol}(\Delta) d^n$. □

For surfaces, we have $n - k = 2$. Hence, the leading term is

$$\frac{(n-2)!}{n!} \left\{ \begin{matrix} n \\ n-2 \end{matrix} \right\} \text{Vol}(\Delta) d^n = \frac{(n-2)(3n-5)}{24} d^n \text{Vol}(\Delta)$$

Therefore, an asymptotically maximal family of T-surfaces $(X_d)_{d \geq 1}$ with polytope Δ must have the following asymptotic number of connected components, as d tends to infinity: $b_0(X_d) \sim \frac{(3n-5)(n-2)}{24} d^n \text{Vol}(\Delta)$.

Corollary 4.16. *There is no family of asymptotically maximal T-surface in Δ for $n = \dim \Delta \geq 65$.*

Proof. Let X_d be a T-surface in $d\Delta$. By Theorem 4.14,

$$b_0(X_d) \leq \frac{7n^2 + 5n + 12}{60} d^n \text{Vol}(\Delta).$$

Thus, for a family of T-surfaces $(X_d)_{d \geq 1}$ to be asymptotically maximal, we must have $\frac{(3n-5)(n-2)}{24} \leq \frac{7n^2 + 5n + 12}{60}$. Reorganizing, we obtain the quadratic inequality $n^2 - 65n + 26 \leq 0$, which is not satisfied for integers greater than or equal to 65. \square

5. CONSTRUCTION OF k -REAL PHASE STRUCTURES

Except in the case of codimensions 0, 1 and n , the description of real phase structure is rather intricate. Even the existence of a real phase structure on the k -skeleton of a unimodular triangulation Γ is not obvious at first sight.

In this section, we explain a construction that produces real phase structures of higher codimension from two real phase structures of lower codimension.

One way to interpret this construction is as a real analogue of stable intersection in tropical geometry. Two tropical varieties Σ_1 and Σ_2 in \mathbb{R}^n may not intersect transversely. However, the Hausdorff limit of $\Sigma_1 \cap (tv + \Sigma_2)$, as t goes to 0, defines a tropical variety, independent of the choice of a generic translation vector v , called the stable intersection of Σ_1 and Σ_2 [MS15, Section 4.3].

Likewise, the classical intersection of two T-manifolds is typically not a manifold. But, locally, if one slightly translates a T-manifold relatively from another, the result will generically be a transverse intersection, but, this time, it is dependent of the direction of translation. In this section, we introduce a combinatorial construction formalizing this idea of stable intersection at the level of real phase structures.

5.1. Stable intersections of real phase structures. Fix a polytope Δ and a unimodular triangulation Γ .

Definition 5.1. A locally acyclic orientation \mathcal{O} on $F_1(\Gamma)$ is an orientation of the graph of edges of Γ such that no simplex of Γ contains an oriented cycle.

For any simplex $\sigma \in \Gamma$, a locally acyclic orientation \mathcal{O} induces an ordering on the vertices of σ by the following rule: for two distinct vertices u and v of σ , $u < v$ if and only if the edge $[u, v]$ is oriented from v to u . This order is well-defined by acyclicity, and it is unique since the graph induced by the simplex σ is complete. From now on, if Γ is a triangulation endowed with a locally acyclic orientation, the notation $\sigma = [v_0, \dots, v_k]$ for a simplex of Γ also implies that $v_0 < \dots < v_n$.

Let $\mathcal{E}_1, \mathcal{E}_2$ be real phase structures on the k_1 and k_2 -skeleton of Γ with $k_1 + k_2 \leq n$, and let \mathcal{O} be a locally acyclic orientation of Γ . We define the $(k_1 + k_2)$ -real phase structure \mathcal{E} as follows. Let $\sigma = [v_0, \dots, v_{k_1+k_2}]$ be a $(k_1 + k_2)$ -simplex of Γ . Set the k_1 -simplex $\sigma_1 = [v_0, v_1, \dots, v_{k_1}]$ and the k_2 -simplex $\sigma_2 = [v_{k_1}, \dots, v_{k_1+k_2}]$. We define:

$$(\mathcal{E}_1 \cap_{\mathcal{O}} \mathcal{E}_2)(\sigma) = \mathcal{E}_1(\sigma_1) \cap \mathcal{E}_2(\sigma_2)$$

Lemma 5.2. *The intersection structure $\mathcal{E} = \mathcal{E}_1 \cap_{\mathcal{O}} \mathcal{E}_2$ defines a $(k_1 + k_2)$ -real phase structure. Moreover, the T-manifold $X_{\mathcal{E}}$ is contained in the intersection $X_{\mathcal{E}_1} \cap X_{\mathcal{E}_2}$.*

Proof. We keep the notation introduced above. Since Γ (and hence σ) is unimodular, $T(\sigma) = T(\sigma_1) \oplus T(\sigma_2)$. Reducing modulo 2 and dualizing, we obtain that $T_2^\perp(\sigma) = T_2^\perp(\sigma_1) \cap T_2^\perp(\sigma_2)$. Since $T_2^\perp(\sigma_1) + T_2^\perp(\sigma_2) = \mathbb{F}_2^n$, the intersection of affine spaces $\mathcal{E}(\sigma) = \mathcal{E}_1(\sigma_1) \cap \mathcal{E}_2(\sigma_2)$ can not be empty, thus it is an affine space directed by $T_2^\perp(\sigma)$, as required.

To verify the parity condition, fix $s \in \mathcal{Q}^n$, and let $\tau = [v_0, v_1, \dots, v_{k_1+k_2+1}]$ be a $(k_1 + k_2 + 1)$ -simplex of Γ . For each $0 \leq i \leq k_1 + k_2 + 1$, let $\sigma_i = [v_0, \dots, \hat{v}_i, \dots, v_{k_1+k_2+1}]$ be the $(k_1 + k_2)$ -simplex opposite to v_i in τ .

By definition of \mathcal{E} , for $0 \leq i \leq k_1$,

$$\mathcal{E}(\sigma_i) = \mathcal{E}_1(\eta_i) \cap \mathcal{E}_2(\gamma_2), \quad \eta_i = [v_0, \dots, \hat{v}_i, \dots, v_{k_1+1}], \quad \gamma_2 = [v_{k_1+1}, \dots, v_{k_1+k_2+1}],$$

and for $k_1 + 1 \leq i \leq k_1 + k_2 + 1$,

$$\mathcal{E}(\sigma_i) = \mathcal{E}_1(\gamma_1) \cap \mathcal{E}_2(\eta_i), \quad \gamma_1 = [v_0, \dots, v_{k_1}], \quad \eta_i = [v_{k_1}, \dots, \hat{v}_i, \dots, v_{k_1+k_2+1}].$$

By the parity condition of \mathcal{E}_1 with the $(k_1 + 1)$ -simplex $[v_0, \dots, v_{k_1+1}]$, there is an even number n_1 of indices i between 0 and k_1 such that $s \in \mathcal{E}_1(\eta_i)$. Similarly, there is an even number n_2 of indices i between $k_1 + 1$ and $k_1 + k_2 + 1$ such that $s \in \mathcal{E}_2(\eta_i)$. So the number of indices i such that $s \in \mathcal{E}(\sigma_i)$ is $\delta_1 n_1 + \delta_2 n_2$, where δ_j is 1 if $s \in \mathcal{E}_j(\gamma_j)$ and 0 otherwise, for $j = 1, 2$. Since this number is even, the parity condition on \mathcal{E} is verified.

Because of the inclusion $\mathcal{E}(\sigma) \subset \mathcal{E}_i(\sigma)$, each cell $C_{\mathcal{E}}(s(\sigma))$ is contained in the cell $C_{\mathcal{E}_i}(s(\sigma))$. This proves the inclusion $X_{\mathcal{E}} \subset X_{\mathcal{E}_1} \cap X_{\mathcal{E}_2}$. \square

Remark 5.3. The binary operations $\cap_{\mathcal{O}}$ on the real phase structures are not commutative. If \mathcal{O}^T is the transposed orientation of \mathcal{O} , then $\mathcal{E}_1 \cap_{\mathcal{O}} \mathcal{E}_2 = \mathcal{E}_2 \cap_{\mathcal{O}^T} \mathcal{E}_1$. Also notice that the unique 0-real phase structure \mathcal{E}_0 is the left and right identity for the operators $\cap_{\mathcal{O}}$.

Theorem 5.4. *Let Γ be triangulation of Δ . For any k between 0 and n , there exists a k -real phase structure on Γ .*

Proof. The existence (and uniqueness) of the 0-real phase structure \mathcal{E}_0 is discussed in example 2.8.

We choose any sign distribution μ on the vertices of Γ , this defines a 1-real phase structure \mathcal{E}_μ (see Example 2.11). We choose any ordering on the vertices of Γ , this defines a globally acyclic orientation \mathcal{O} by orienting each edge from the smallest endpoint to the largest. For any k between 1 and n , we construct inductively the k -real phase structure $\mathcal{E}_k = \mathcal{E}_{k-1} \cap_{\mathcal{O}} \mathcal{E}_\mu$. \square

Not all real phase structures can be obtained by the operators $\cap_{\mathcal{O}}$. Stronger than that, there exists T-manifolds that are not contained in any other T-manifold except themselves and the full T-manifold of codimension 0. Figure 7 shows such a 2-real phase structure \mathcal{E}_S on a polygon Δ_S . For each triangle τ of Δ_S , the set $\mathcal{E}_S(\tau)$ is a singleton in $\mathcal{Q}^2 = \{++, +-, -+, --\}$, displayed directly on τ on the figure. It is impossible to extend it such that the T-curve contains the 10 points of $X_{\mathcal{E}_S}$. Indeed, if one starts by fixing the 1-real phase structure on the edge joining the two interior vertices, the structure \mathcal{E}_S will impose how to extend the 1-real phase structure on the adjacent edges. But this local spreading conditions are not consistent globally and the T-curve will always miss at least one of the ten points.

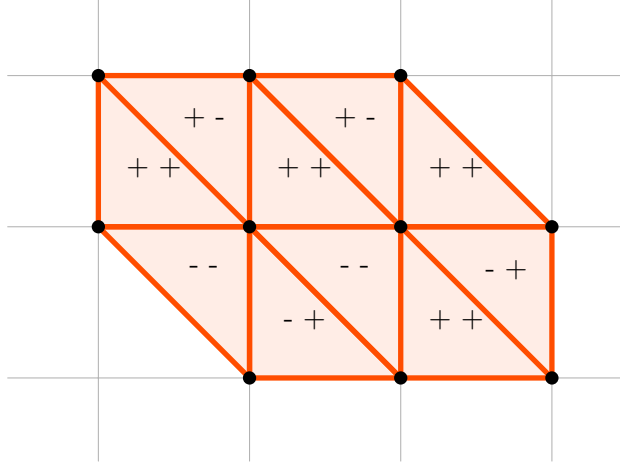


FIGURE 7. The polygon Δ_S with the real phase structure on the 2-skeleton \mathcal{E}_S

5.2. Description for T-manifold of codimension 2. When $k_1 = k_2 = 1$, the real phase structure \mathcal{E}_1 and \mathcal{E}_2 can be encoded by sign distributions μ_1 and μ_2 (see Example 2.11). In this situation, the description of $\mathcal{E} = \mathcal{E}_1 \cap_{\mathcal{O}} \mathcal{E}_2$ becomes especially simple: it is entirely described by the two sign distributions and the locally acyclic orientation.

As in classical combinatorial patchworking for T-hypersurfaces, all the data can be drawn directly on the triangulation, and there is a straightforward rule for constructing the T-manifold of codimension 2 from these data. This makes this description of these T-manifolds of codimension 2 especially easy to present and manipulate. In particular, it is a convenient way to produce T-curves in 3-dimensional space, and we will use it in Section 6 to construct maximal curves.

Let τ be a triangle of $\tilde{\Gamma}$ with vertices v_0, v_1 and v_2 ordered by \mathcal{O} . We call τ a *compatible triangle* if $\mu_1(v_0) \neq \mu_1(v_1)$ and $\mu_2(v_1) \neq \mu_2(v_2)$. Equivalently, along the two consecutive edges with the same orientation, the endpoints of the first edge differ for the sign distribution μ_1 , and the endpoints of the second differ for μ_2 .

Figure 8 presents four acyclic triangles with twice the same sign distribution $\mu_1 = \mu_2$ (represented by the color of the vertices). Only the top-left triangle is compatible.

By Lemma 5.2, the set $\mathcal{E}(\tau) = \{s \in \mathcal{Q}^3 \mid s(\tau)\}$ is a compatible triangle} is exactly the 2-real phase structure $\mathcal{E}_1 \cap_{\mathcal{O}} \mathcal{E}_2$. Moreover, the T-manifold $X_{\mathcal{E}}$ is contained in the intersection of the two T-hypersurfaces define by μ_1 and μ_2 .

Example 5.5. Figure 9 illustrates a part of the patchwork in a single triangle. The color of the upper half of the vertices of the triangle represents the first distribution of sign associated the orange T-curve. The color of the lower half of the vertices of the triangle represents the second distribution of sign associated the green T-curve. The T-manifold of codimension 2, which here is only a point, is represented in yellow.

In this setting, we have the following realizability theorem for T-manifold of codimension 2.

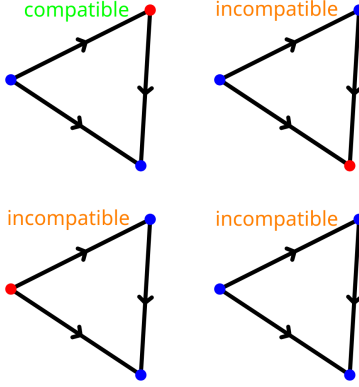


FIGURE 8. Compatible and incompatible triangles

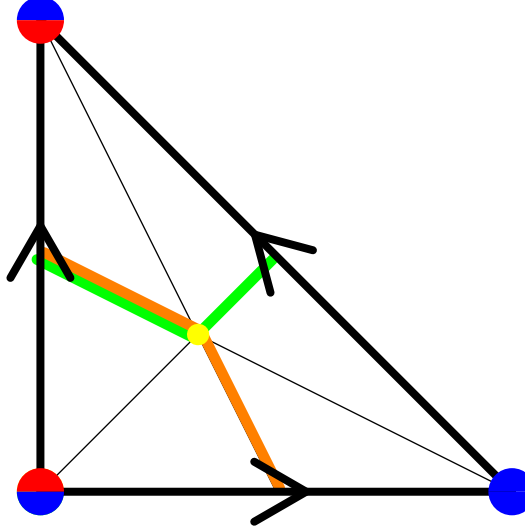


FIGURE 9. Illustration of the real stable intersection

Theorem 5.6. *Let Δ be a smooth lattice polytope, Γ be a convex triangulation of Δ , \mathcal{O} a globally acyclic orientation of Γ and two sign distributions μ_1, μ_2 . There exists two hypersurfaces H_1 and H_2 with Newton polytope Δ in $\mathbb{R}X_\Delta$ such that, for any $i = 1, 2$, the triple $(\mathbb{R}X_\Delta, H_i, H_1 \cap H_2)$ is homeomorphic to $(\tilde{\Delta}, X_{\mathcal{E}_{\mu_i}}, X_{\mathcal{E}_{\mu_1} \cap \mathcal{O} \mathcal{E}_{\mu_2}})$. This homeomorphism is stratified in the sense of Theorem 2.15.*

The proof of this theorem is developed in the following subsection and is based on Sturmfels' patchworking theorem.

5.3. Proof of Theorem 5.6.

5.3.1. *Sturmfels' patchworking of complete intersection.* There is another distinct approach to define intersection of T-hypersurfaces. Sturmfels had generalized Viro's theorem to complete intersections of any number of T-hypersurface [Stu94]. Here

we extend Sturmfels' construction for any two real phase structures and then restate its theorem for complete intersection of two T-hypersurfaces.

Fix two polytopes $\Delta^{(1)}$ and $\Delta^{(2)}$ with respective subdivisions $\Gamma^{(1)}$ and $\Gamma^{(2)}$. Consider a subdivision Γ of the Minkowski sum $\Delta = \Delta^{(1)} + \Delta^{(2)}$. The subdivision Γ is called *mixed* if each cell γ of Γ can be decomposed in the form $\gamma_1 + \gamma_2$, where $\gamma_1 \in \Gamma^{(1)}$ and $\gamma_2 \in \Gamma^{(2)}$, and this decomposition is compatible with intersection: if $\gamma = \gamma_1 + \gamma_2$ and $\gamma' = \gamma'_1 + \gamma'_2$, then $\gamma \cap \gamma' = (\gamma_1 \cap \gamma'_1) + (\gamma_2 \cap \gamma'_2)$.

If, in addition, for each cell, $\dim \gamma = \dim \gamma_1 + \dim \gamma_2$ then the mixed subdivision Γ is said to be *fine*.

A mixed subdivision Γ of $\Delta = \Delta^{(1)} + \Delta^{(2)}$ is called *coherent* if there are heights functions $\nu_i: F_0(\Gamma^{(i)}) \rightarrow \mathbb{R}$ such that $\Gamma^{(1)}$, $\Gamma^{(2)}$ and Γ are respectively the convex subdivisions Γ_{ν_1} , Γ_{ν_2} and $\Gamma_{\nu_1 \oplus \nu_2}$ where

$$\nu_1 \oplus \nu_2(x) := \min\{\nu_1(x_1) + \nu_2(x_2) \mid x_1 \in \Delta^{(1)}, x_2 \in \Delta^{(2)} \text{ and } x_1 + x_2 = x\}.$$

Now suppose $\Gamma^{(1)}$ and $\Gamma^{(2)}$ are both (non necessarily convex) triangulations equipped with real phase structures $\mathcal{E}^{(1)}$ and $\mathcal{E}^{(2)}$ respectively. Let Γ be a fine mixed subdivision of $\Gamma^{(1)}$ and $\Gamma^{(2)}$.

As in Section 2, extend by symmetry the mixed subdivision Γ of Δ into the subdivision $\tilde{\Gamma}$ of $\tilde{\Delta}$. Fix $i = 1$ or 2 . Consider simplices $s(\gamma) \in \tilde{\Gamma}$ with $\gamma = \gamma_1 + \gamma_2$, where $\gamma_1 \in \Gamma^{(1)}$ and $\gamma_2 \in \Gamma^{(2)}$, such that $s \in \mathcal{E}^{(i)}(\gamma_i)$. We define $Y_{\Gamma, \mathcal{E}^{(i)}}$ to be the full subcomplex of $\text{Bar}(\tilde{\Gamma})$ consisting of the barycenters of such simplices $s(\gamma)$.

Sturmfels' result can be restated as follows:

Theorem 5.7. *Let $\Delta^{(1)}, \Delta^{(2)}$ be a lattice polytopes, $\Gamma_{\nu_1 \oplus \nu_2}$ a coherent fine mixed subdivision of $\Delta = \Delta^{(1)} + \Delta^{(2)}$ and $\mathcal{E}^{(1)}, \mathcal{E}^{(2)}$ real phase structures of codimension 1 respectively on $\Delta^{(1)}, \Delta^{(2)}$. There exists algebraic hypersurfaces H_1, H_2 with respective Newton polytopes $\Delta^{(1)}, \Delta^{(2)}$ in $\mathbb{R}X_\Delta$ and a homeomorphism $h: \tilde{\Delta} \rightarrow \mathbb{R}X_\Delta$ such that $H_1 \cap H_2$ is a smooth complete intersection and $h(Y_{\Gamma_{\nu_1 \oplus \nu_2}, \mathcal{E}^{(i)}}) = H_i$, for $i = 1, 2$. The homeomorphism h is stratified in the sense of Theorem 2.15.*

For $i = 1, 2$, let μ_i be a sign distribution such that $\mathcal{E}^{(i)} = \mathcal{E}_{\mu_i}$ (see Example 2.11). The hypersurfaces H_i are given by the zero sets $\{P_t^{(i)} = 0\} \subset \mathbb{R}X_\Delta$, for sufficiently small $t > 0$, of the Viro polynomials

$$P_t^{(i)}(x) = \sum_{a \in F_0(\Gamma_{\nu_i})} \mu_i(a) t^{\nu_i(a)} x^a.$$

Example 5.8. Figure 10 illustrates a part of the Sturmfels' construction. For each vertex $u = u_1 + u_2$ of the mixed subdivision the upper half represents $\mu_1(u_1)$ while the lower half represents $\mu_2(u_2)$. The curve $Y_{\Gamma, \mathcal{E}_1}$ is represented in orange. The curve $Y_{\Gamma, \mathcal{E}_2}$ is represented in green. The intersection $Y_{\Gamma, \mathcal{E}_1} \cap Y_{\Gamma, \mathcal{E}_2}$, which here is only a point, is represented in yellow.

5.3.2. From Sturmfels' method to 2-real phases structures. A locally acyclic orientation defines a mixed subdivision of $2\Delta = \Delta + \Delta$ as follows. Inside 2Δ there is a triangulation 2Γ made of the simplices $2\tau = \tau + \tau$ with $\tau \in \Gamma$. For each n -simplex $\tau = [v_0, v_1, \dots, v_n]$ ordered by \mathcal{O} , we subdivide 2τ by the $n+1$ mixed cells $[v_0, v_1, \dots, v_j] + [v_j, v_{j+1}, \dots, v_n]$ for $j = 0, 1 \dots n$. All these mixed cells formed the fine mixed subdivision $\Gamma_{\mathcal{O}}$ of 2Δ .

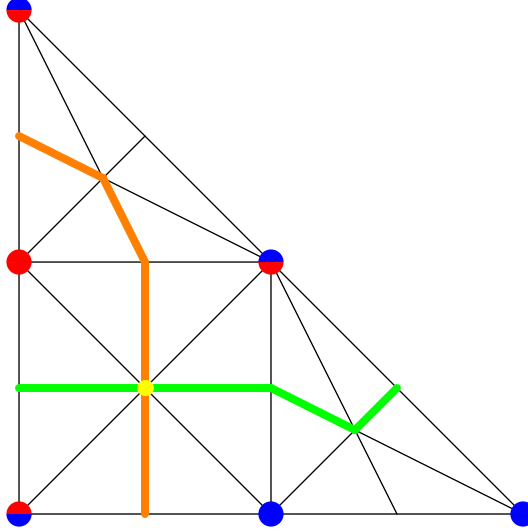


FIGURE 10. Illustration of Sturmfels's patchworking method

Proposition 5.9. *Let Γ be a triangulation. The map $\mathcal{O} \mapsto \Gamma_{\mathcal{O}}$ defines a bijection between locally acyclic orientation of Γ and fine mixed subdivision refining 2Γ . Moreover, the mixed subdivision $\Gamma_{\mathcal{O}}$ is coherent if and only if \mathcal{O} is globally acyclic and Γ is convex.*

Proof. After using the Cayley trick, this is the Lemma 7.2.9 of [DLRS10]. \square

If we give ourselves two sign distributions $\mu_1, \mu_2: F_0(\Gamma) \rightarrow \{-, +\}$, we can create two manifolds of codimension 2:

- the intersection $Y_{\Gamma_{\mathcal{O}}, \mathcal{E}_{\mu_1}} \cap Y_{\Gamma_{\mathcal{O}}, \mathcal{E}_{\mu_2}}$ obtained by Sturmfels' method
- the T-manifold $X_{\mathcal{E}}$ associated to the 2-real phase structure $\mathcal{E} = \mathcal{E}_{\mu_1} \cap_{\mathcal{O}} \mathcal{E}_{\mu_2}$.

These two constructions are strongly related by the following theorem:

Theorem 5.10. *Let Δ be a smooth lattice polytope, Γ be a triangulation of Δ , \mathcal{O} a locally acyclic orientation of Γ and two real phase structures $\mathcal{E}_1, \mathcal{E}_2$ of codimension 1 on Γ . For any $i = 1, 2$, the triples of topological spaces $(\widetilde{\Delta}, X_{\mathcal{E}_i}, X_{\mathcal{E}_1 \cap_{\mathcal{O}} \mathcal{E}_2})$ and $(2\widetilde{\Delta}, Y_{\Gamma_{\mathcal{O}}, \mathcal{E}_i}, Y_{\Gamma_{\mathcal{O}}, \mathcal{E}_1} \cap Y_{\Gamma_{\mathcal{O}}, \mathcal{E}_2})$ are homeomorphic. This homeomorphism is stratified in the sense of Theorem 2.15.*

The proof of this theorem will need the following topological result:

Theorem 5.11 (Weak Schoenflies PL theorem, [New60, Bro62]). *Let M be a PL sphere of dimension n . For any PL sphere N of dimension $n-1$ in M , the set $M \setminus N$ is made of two connected components, whose closures are topological n -balls.*

Proof of Theorem 5.10. We fix μ_1 and μ_2 signs distributions associated to \mathcal{E}_1 and \mathcal{E}_2 . Recall that, by Remark 5.3, the role of \mathcal{E}_1 and \mathcal{E}_2 can be interchanged. Thus, we only need to exhibit one of the two homeomorphisms.

The proof proceeds by constructing regular cell subdivisions \mathcal{C} of $\widetilde{\Delta}$ and \mathcal{D} of $2\widetilde{\Delta}$ adapted to the respective triples and combinatorially isomorphic. This will directly

yield our result since the combinatoric of regular cell complexes determines them up to cellular homeomorphism.

We begin by defining the regular cell decomposition \mathcal{C} of $\tilde{\Delta}$ with subcomplexes \mathcal{C}' and \mathcal{C}'' that subdivide $X_{\mathcal{E}_1}$ and $X_{\mathcal{E}_1 \cap_{\mathcal{O}} \mathcal{E}_2}$, respectively. The decomposition \mathcal{C} refines $\tilde{\Delta}$ and is coarser than $\text{Bar } \tilde{\Delta}$. Each simplex $\sigma \in \tilde{\Gamma}$ intersecting $X_{\mathcal{E}_1}$ is divided in two by the T-hypersurface, and $X_{\mathcal{E}_1}$ is, in turn, divided in two by $X_{\mathcal{E}_1 \cap_{\mathcal{O}} \mathcal{E}_2}$, if they intersect. We define

$$\mathcal{C} := \{\mathcal{C}(\sigma)^+, \mathcal{C}(\sigma)^-, \mathcal{C}'(\sigma)^+, \mathcal{C}'(\sigma)^-, \mathcal{C}''(\sigma) \mid \sigma \in \tilde{\Gamma}\}$$

with the following definitions:

$$\begin{aligned} \mathcal{C}(\sigma)^{\pm} &:= \bigcup_{\substack{u=\tau_0 < \dots < \tau_n = \sigma \\ \mu_1(u) = \pm}} [\hat{\tau}_0, \dots, \hat{\tau}_n], \\ \mathcal{C}'(\sigma)^{\pm} &:= \bigcup_{\substack{[u,v] = \tau_1 < \dots < \tau_n = \sigma \\ \mu_1(u) \neq \mu_1(v) \\ \mu_2(u) = \pm}} [\hat{\tau}_1, \dots, \hat{\tau}_n] \end{aligned}$$

and

$$\mathcal{C}''(\sigma) = \bigcup_{\substack{[u,v,w] = \tau_2 < \dots < \tau_n = \sigma \\ \mu_1(u) \neq \mu_1(v) \\ \mu_2(v) \neq \mu_2(w)}} [\hat{\tau}_2, \dots, \hat{\tau}_n] = C_{\mathcal{E}_1 \cap_{\mathcal{O}} \mathcal{E}_2}(\sigma).$$

Note that some of that cells might be empty. First observe that the

$$\mathcal{C}(\sigma)^+ \cup \mathcal{C}(\sigma)^- = \bigcup_{\tau_0 < \dots < \tau_n = \sigma} [\hat{\tau}_0, \dots, \hat{\tau}_n] = \sigma$$

and

$$\mathcal{C}'(\sigma)^+ \cup \mathcal{C}'(\sigma)^- = \bigcup_{\substack{[u,v] = \tau_1 < \dots < \tau_n = \sigma \\ \mu_1(u) \neq \mu_1(v)}} [\hat{\tau}_1, \dots, \hat{\tau}_n] = C_{\mathcal{E}_1}(\sigma).$$

Secondly,

$$\mathcal{C}(\sigma)^+ \cap \mathcal{C}(\sigma)^- = \bigcup_{\substack{[u,v] = \tau_1 < \dots < \tau_n = \sigma \\ \mu_1(u) \neq \mu_1(v)}} [\hat{\tau}_1, \dots, \hat{\tau}_n] = C_{\mathcal{E}_1}(\sigma)$$

and

$$\mathcal{C}'(\sigma)^+ \cap \mathcal{C}'(\sigma)^- = \bigcup_{\substack{[u,v,w] = \tau_2 < \dots < \tau_n = \sigma \\ \mu_1(v) \neq \mu_1(w) \\ \mu_2(u) \neq \mu_2(v)}} [\hat{\tau}_1, \dots, \hat{\tau}_n] = C_{\mathcal{E}_1 \cap_{\mathcal{O}} \mathcal{E}_2}(\sigma).$$

To justify the first equality of the last line, observe that given a triangle $[u, v, w]$ with two edges $[u_1, v_1]$ and $[u_2, v_2]$ such that $\mu_1(u_1) \neq \mu_1(v_1)$, $\mu_1(u_2) \neq \mu_1(v_2)$, $\mu_2(u_1) = +$ and $\mu_2(u_2) = -$, we have either $u_1 < u_2$ or $u_2 < u_1$. Then either $u = u_1 < v = u_2 < w = v_2$ or $u = u_2 < v = u_1 < w = v_1$ and, in both case, $\mu_2(u) \neq \mu_2(v)$ and $\mu_1(v) \neq \mu_1(w)$.

Let's also define

$$\underline{\mathcal{C}(\sigma)^\pm} := \bigcup_{\substack{u=\tau_0 < \dots < \tau_{n-1} < \sigma \\ \mu_1(u) = \pm}} [\hat{\tau}_0, \dots, \hat{\tau}_{n-1}] = C(\sigma)^\pm \cap \partial\sigma.$$

Observe that

$$\underline{\mathcal{C}(\sigma)^+} \cap \underline{\mathcal{C}(\sigma)^-} = \bigcup_{\substack{\tau_1 < \dots < \tau_{n-1} < \sigma \\ \tau_1 = [u, v], \mu_1(u) \neq \mu_1(v)}} [\hat{\tau}_1, \dots, \hat{\tau}_{n-1}] = \partial C_{\mathcal{E}_1}(\sigma).$$

Suppose $C_{\mathcal{E}_1}(\sigma)$ is non-empty. We apply the weak PL Schoenflies theorem to the pair $(\partial\sigma, \partial C_{\mathcal{E}_1}(\sigma))$, which are both PL spheres of respective dimension $n-1$ and $n-2$ (the first by definition of PL sphere and the second by Proposition 2.5). The two closures $\underline{\mathcal{C}(\sigma)^\pm}$ of the connected components are $(n-1)$ -balls. Taking the cone over the barycenter of σ , we recover the cells

$$\mathcal{C}(\sigma)^\pm = \bigcup_{\substack{u=\tau_0 < \dots < \tau_n = \sigma \\ \mu_1(u) = \pm}} [\hat{\tau}_0, \dots, \hat{\tau}_n] = \text{Cone}_{\hat{\sigma}}(\underline{\mathcal{C}(\sigma)^\pm})$$

which thus are n -balls.

Now we similarly subdivide $\partial C_{\mathcal{E}_1}(\sigma)$:

$$\underline{\mathcal{C}'(\sigma)^\pm} := \bigcup_{\substack{[u, v] = \tau_1 < \dots < \tau_{n-1} < \sigma \\ \mu_1(u) \neq \mu_1(v) \\ \mu_2(u) = \pm}} [\hat{\tau}_1, \dots, \hat{\tau}_{n-1}] = \mathcal{C}'(\sigma)^\pm \cap \partial\sigma \subset \partial C_{\mathcal{E}_1}(\sigma).$$

Observe that

$$\underline{\mathcal{C}'(\sigma)^+} \cap \underline{\mathcal{C}'(\sigma)^-} = \bigcup_{\substack{[u, v, w] = \tau_2 < \dots < \tau_{n-1} < \sigma \\ \mu_1(v) \neq \mu_1(w) \\ \mu_2(u) \neq \mu_2(v)}} [\hat{\tau}_1, \dots, \hat{\tau}_{n-1}] = \partial C_{\mathcal{E}_1 \cap \mathcal{E}_2}(\sigma).$$

Suppose $C_{\mathcal{E}_1 \cap \mathcal{E}_2}(\sigma)$ is non-empty. We apply weak PL Schoenflies theorem again to $(\partial C_{\mathcal{E}_1}(\sigma), \partial C_{\mathcal{E}_1 \cap \mathcal{E}_2}(\sigma))$. Indeed, $\partial C_{\mathcal{E}_1 \cap \mathcal{E}_2}(\sigma)$ and $\partial C_{\mathcal{E}_1}(\sigma)$ are both PL spheres of respective dimension $n-2$ and $n-3$ by Proposition 2.5. Thus, the closures $\underline{\mathcal{C}'(\sigma)^\pm}$ of the two components of $\partial C_{\mathcal{E}_1}(\sigma) \setminus \partial C_{\mathcal{E}_1 \cap \mathcal{E}_2}(\sigma)$ are $(n-2)$ -balls. Taking the cone over the barycenter of σ , we recover the cells of \mathcal{C}

$$\mathcal{C}'(\sigma)^\pm = \bigcup_{\substack{u=\tau_0 < \dots < \tau_n = \sigma \\ \mu_1(u) = \pm}} [\hat{\tau}_0, \dots, \hat{\tau}_n] = \text{Cone}_{\hat{\sigma}}(\underline{\mathcal{C}'(\sigma)^\pm})$$

that are thus $(n-1)$ -balls.

Since $\mathcal{C}''(\sigma) = C_{\mathcal{E}_1 \cap \mathcal{E}_2}(\sigma)$ is an $(n-2)$ -ball, all the cells of \mathcal{C} are balls.

We verify that the boundary of each cell is a union of cells:

$$\partial \mathcal{C}(\sigma)^\pm = \underline{\mathcal{C}(\sigma)^\pm} \cup C_{\mathcal{E}_1}(\sigma) = \bigcup_{\tau < \sigma} \mathcal{C}(\tau)^\pm \cup \mathcal{C}'(\sigma)^+ \cup \mathcal{C}'(\sigma)^-,$$

$$\partial \mathcal{C}'(\sigma)^\pm = \underline{\mathcal{C}'(\sigma)^\pm} \cup C_{\mathcal{E}_1 \cap \mathcal{E}_2}(\sigma) = \bigcup_{\tau < \sigma} \mathcal{C}'(\tau)^\pm \cup \mathcal{C}''(\sigma),$$

and

$$\partial \mathcal{C}''(\sigma) = \bigcup_{\tau < \sigma} \mathcal{C}''(\tau).$$

Finally, since the interior of each simplex of the barycentric subdivision $\text{Bar}(\tilde{\Gamma})$ lies in the interior of a unique cell of \mathcal{C} , any point $x \in \tilde{\Delta}$ lies in the interior of one cell of \mathcal{C} . It follows that \mathcal{C} is a regular cell subdivision of $\tilde{\Delta}$ with subcomplexes $\mathcal{C}' = \{\mathcal{C}'(\sigma)^+, \mathcal{C}'(\sigma)^-, \mathcal{C}''(\sigma) : \sigma \in \tilde{\Gamma}\}$ subdividing $X_{\mathcal{E}_1}$ and $\mathcal{C}'' = \{\mathcal{C}''(\sigma) : \sigma \in \tilde{\Gamma}\}$ subdividing $X_{\mathcal{E}_1 \cap_{\mathcal{O}} \mathcal{E}_2}$ (with the canonical cell decomposition).

On the other hand, we have a refinement \mathcal{D} of the triangulation $\tilde{2\Gamma}$ of $\tilde{2\Delta}$ defines using the two T-hypersurfaces $Y_{\Gamma_{\mathcal{O}}, \mathcal{E}_1}$ and $Y_{\Gamma_{\mathcal{O}}, \mathcal{E}_2}$ given by Sturmfels' method. In a simplex $\sigma \in \tilde{\Gamma}$, each T-hypersurface divides $2\sigma \in \tilde{2\Gamma}$ in two halves:

$$M_i(\sigma)^{\pm} := \bigcup_{\substack{u_1+u_2=\tau_0 < \dots < \tau_n \subset 2\sigma \\ \mu_i(u_i)=\pm}} [\hat{\tau}_0, \dots, \hat{\tau}_n]$$

such that $M_i(\sigma)^+ \cap M_i(\sigma)^- = Y_{\Gamma_{\mathcal{O}}, \mathcal{E}_i} \cap \sigma$.

We define

$$\mathcal{D} = \{\mathcal{D}(\sigma)^+, \mathcal{D}(\sigma)^-, \mathcal{D}'(\sigma)^+, \mathcal{D}'(\sigma)^-, \mathcal{D}''(\sigma) : 2\sigma \in \tilde{2\Gamma}\}$$

with

$$\begin{aligned} \mathcal{D}(\sigma)^{\pm} &:= M_1(\sigma)^{\pm}, \\ \mathcal{D}'(\sigma)^{\pm} &:= M_1(\sigma)^+ \cap M_1(\sigma)^- \cap M_2(\sigma)^{\pm} \end{aligned}$$

and

$$\mathcal{D}''(\sigma) := M_1(\sigma)^+ \cap M_1(\sigma)^- \cap M_2(\sigma)^+ \cap M_2(\sigma)^-.$$

Here we use Sturmfels' theorem to see that each cell of \mathcal{D} is topological ball. Indeed, for any simplex, the mixed subdivision $\sigma_{\mathcal{O}}$ of 2σ is always coherent and fine. Thus, by applying Sturmfels theorem and considering only the positive orthant $Q^+ = \{[u_0, \dots, u_n], u_i \geq 0\} \subset \mathbb{R}P^n$ we have two linear forms l_1 and l_2 and a homeomorphism $h: 2\sigma \rightarrow Q^+$ such that $h(\mathcal{D}(\sigma)^{\pm}) = \{\pm l_1 \geq 0\}$, $h(\mathcal{D}'(\sigma)^{\pm}) = \{l_1 = 0\} \cap \{\pm l_2 \geq 0\}$ and $h(\mathcal{D}''(\sigma)) = \{l_1 = 0\} \cap \{l_2 = 0\}$. Thus, all the cells are homeomorphic to polyhedron and in particular to topological balls.

By construction $\mathcal{D}' = \{\mathcal{D}(\sigma)^-, \mathcal{D}'(\sigma)^+, \mathcal{D}'(\sigma)^-, \mathcal{D}''(\sigma) : \sigma \in \tilde{2\Gamma}\}$ is a subdivision of $Y_{\Gamma_{\mathcal{O}}, \mathcal{E}_1}$ and $\mathcal{D}'' = \{\mathcal{D}''(\sigma) : \sigma \in \tilde{2\Gamma}\}$ of $Y_{\Gamma_{\mathcal{O}}, \mathcal{E}_1} \cap Y_{\Gamma_{\mathcal{O}}, \mathcal{E}_2}$. We also deduce the following boundaries:

$$\partial \mathcal{D}(\sigma)^{\pm} = \bigcup_{\tau < \sigma} \mathcal{D}(\tau)^{\pm} \cup \mathcal{D}'(\sigma)^+ \cup \mathcal{D}'(\sigma)^-,$$

$$\partial \mathcal{D}'(\sigma)^{\pm} = \bigcup_{\tau < \sigma} \mathcal{D}'(\tau)^{\pm} \cup \mathcal{D}''(\sigma),$$

and

$$\partial \mathcal{D}''(\sigma) = \bigcup_{\tau < \sigma} \mathcal{D}''(\tau).$$

fhigbonmk

The map

$$f: \mathcal{C} \longrightarrow \mathcal{D}$$

defined by

$$f(\mathcal{C}(\sigma)^{\pm}) = \mathcal{D}(\sigma)^{\pm}, \quad f(\mathcal{C}'(\sigma)^{\pm}) = \mathcal{D}'(\sigma)^{\pm}, \quad f(\mathcal{C}''(\sigma)) = \mathcal{D}''(\sigma)$$

is a bijection preserving inclusions. It induces a homeomorphism $h: \tilde{\Delta} \rightarrow \tilde{2\Delta}$ such that a cell of \mathcal{C} is sent on the corresponding cell of \mathcal{D} (see [BLVS⁺99, Corollary 4.7.9]). In particular, h maps $X_{\mathcal{E}_1}$ onto $Y_{\Gamma_{\mathcal{O}}, \mathcal{E}_1}$ and $X_{\mathcal{E}_1 \cap_{\mathcal{O}} \mathcal{E}_2}$ onto $Y_{\Gamma_{\mathcal{O}}, \mathcal{E}_1} \cap Y_{\Gamma_{\mathcal{O}}, \mathcal{E}_2}$.

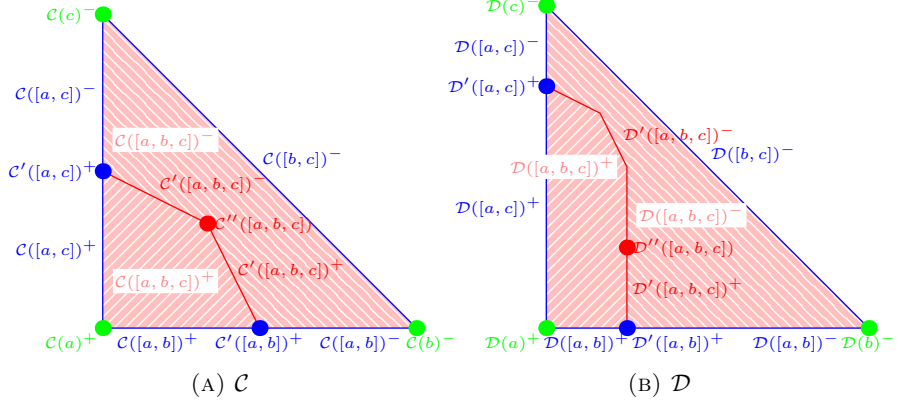


FIGURE 11. Illustration of the two regular cell decompositions of the proof on a triangle $[a, b, c]$

In addition, since $h(\sigma) = 2\sigma$ for any simplex $\sigma \in \tilde{\Gamma}$, the homeomorphism h is stratified. \square

Proof of Theorem 5.6. Since $\Gamma_{\mathcal{O}}$ is a coherent fine mixed subdivision thanks to Proposition 5.9, Sturmfels' theorem gives the existence of algebraic hypersurfaces $H_1, H_2 \subset \mathbb{R}X_{\Delta}$ such that, for any $i = 1, 2$, $(\mathbb{R}X_{\Delta}, H_i, H_1 \cap H_2)$ and $(\tilde{\Delta}, Y_{\Gamma_{\mathcal{O}}, \mathcal{E}_i}, Y_{\Gamma_{\mathcal{O}}, \mathcal{E}_1} \cap Y_{\Gamma_{\mathcal{O}}, \mathcal{E}_2})$ are homeomorphic. By Theorem 5.10, there is a homeomorphism between $(\tilde{\Delta}, X_{\mathcal{E}_i}, X_{\mathcal{E}_1 \cap \mathcal{E}_2})$ and $(\tilde{\Delta}, Y_{\Gamma_{\mathcal{O}}, \mathcal{E}_i}, Y_{\Gamma_{\mathcal{O}}, \mathcal{E}_1} \cap Y_{\Gamma_{\mathcal{O}}, \mathcal{E}_2})$. The composition of the two homeomorphisms, that both respect the stratification, gives the desired result. \square

5.4. The case of T-curve in dimension 3. The goal of this subsection is to study the local combinatorics of T-curves obtained by applying the "stable intersection" method in dimension 3. The results will be used for the analysis of the T-curves in the next section.

Let (Δ, Γ) be a 3-dimensional triangulated polytope, μ a sign distribution and \mathcal{O} a locally acyclic orientation. We consider the T-curve $X_{\mathcal{E}}$ where $\mathcal{E} = \mathcal{E}_{\mu} \cap_{\mathcal{O}} \mathcal{E}_{\mu}$.

In a tetrahedron σ of $\tilde{\Gamma}$, either $X_{\mathcal{E}}$ does not meet σ or it intersects two faces of σ . In the latter case, we call the common edge of the two faces the axis of $X_{\mathcal{E}}$ in σ .

For the tetrahedron $\sigma = [v_0, v_1, v_2, v_3]$, with the vertices ordered by \mathcal{O} , the Table 1 summarizes the possible axis of $X_{\mathcal{E}}$ according to the sign distribution μ on the vertices of σ . When $X_{\mathcal{E}}$ does not intersect σ , the axis is indicated as "none" (empty octant). It suffices to record the cases where $\mu(v_0) = +$, since inverting all signs does not change the real phase structure.

We illustrate one case in Figure 12. Here we represent the configuration corresponding to the fifth line of the table: the axis of $X_{\mathcal{E}}$ is the edge $[v_0, v_1]$ (in grey). The sign of a vertex is represented by its color (blue or red).

Proposition 5.12. *Let $\sigma = [v_0, v_1, v_2, v_3]$ be a tetrahedron in Γ with vertices ordered by \mathcal{O} . Let e be one of the edges $[v_0, v_1]$, $[v_1, v_2]$, $[v_2, v_3]$ or $[v_3, v_0]$. There exists a unique octant $s \in \mathbb{Q}^3$ such that $s(e)$ is the axis of $X_{\mathcal{E}}$ in $s(\sigma)$.*

Proof. Since σ is unimodular, each of the eight distributions of signs on four vertices (up to inversion of all the signs) appear on exactly one of the eight copies of σ (see

v_0	v_1	v_2	v_3	axis
+	+	+	+	none
+	+	+	-	none
+	+	-	+	$[v_2, v_3]$
+	+	-	-	none
+	-	+	+	$[v_0, v_1]$
+	-	+	-	$[v_1, v_2]$
+	-	-	+	$[v_0, v_3]$
+	-	-	-	none

TABLE 1. Possible axis of the T-curve $X_{\mathcal{E}}$ in a tetrahedron σ , depending on the sign distribution

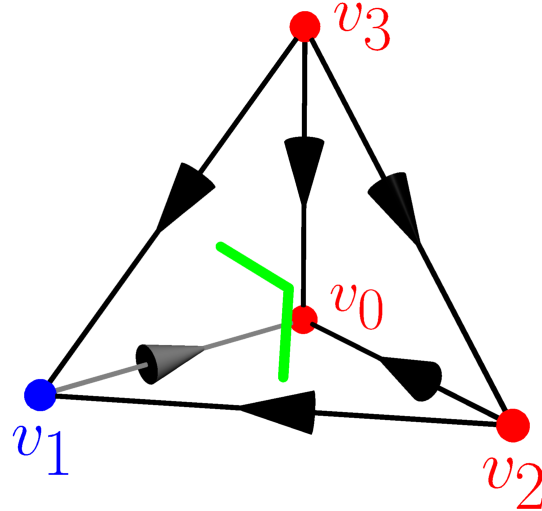


FIGURE 12. Local configuration of the T-curve $X_{\mathcal{E}}$ in $[v_0, v_1, v_2, v_3]$ corresponding to the fifth line of table 1

[Dem24] Lemma 1.3.3). As shown by Table 1, one of these sign distributions is such that the corresponding copy of e is the axis of $X_{\mathcal{E}}$ in the corresponding copy of σ . \square

6. MAXIMAL CURVE IN CODIMENSION 2

Here we describe, for any positive integer d , a pair (Σ_d, C_d) of maximal T-surface and maximal T-curve with Newton polytope $d\Delta_3$. For this, we use the method of Section 5. They will correspond, by Theorem 5.6, to a maximal real algebraic surfaces of degree d and maximal real algebraic curve in $\mathbb{R}P^3$.

In this section, we fix $d \geq 1$ and $\Delta = d\Delta_3$ inside \mathbb{R}^3 with coordinate (x, y, z) .

6.1. Triangulation. We describe the standard floor triangulation of the tetrahedron Δ . For each integer k such that $0 \leq k \leq d$, define the slice $T_k = \Delta \cap \{z = d - k\}$.

We give the following triangulation to the slices T_k .

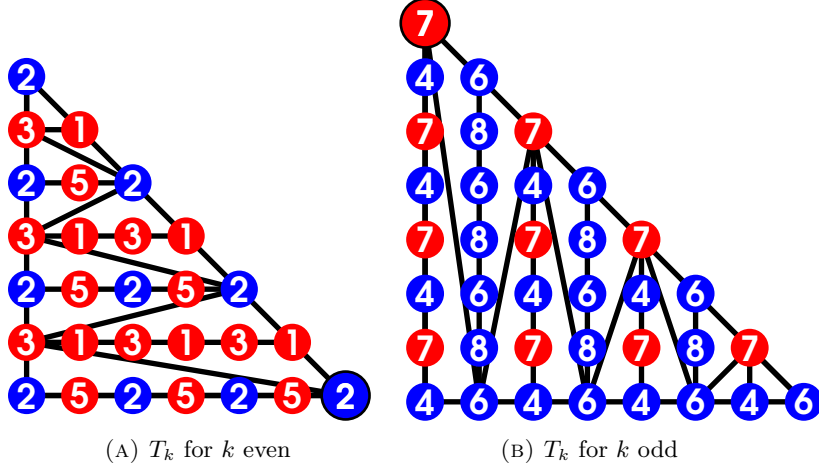


FIGURE 13. The coarse triangulation of T_k and the parities of the vertices

For even k , we subdivide T_k by the segments $S_k^l = T_k \cap \{y = k - l\}$ for $0 \leq l \leq k$ and the diagonals between the points $(k, 2m, d - k)$ and $(0, 1 + 2m, d - k)$ for $0 \leq 2m \leq k$ (see Figure 13a).

For odd k , we subdivide T_k by the segments $S_k^l = T_k \cap \{x = k - l\}$ for $0 \leq l \leq k$ and the diagonals between the points $(2m, k - 2m, d - k)$ and $(1 + 2m, 0, d - k)$ for $0 \leq 2m \leq k$ (see Figure 13b).

The triangulation of each T_k can be uniquely refined in a unimodular triangulation.

Now, we use the triangulation of T_k to define the triangulation of Δ .

For even k , take the cone of T_k and its triangulation over $(0, k + 1, d - k - 1)$, provided that $k + 1 < d$, and the cone over $(0, k - 1, d - k + 1)$, provided that $k > 0$.

For odd k , take the cones of T_k and its triangulation over $(k + 1, 0, d - k - 1)$, provided that $k + 1 < d$, and the cone over $(k - 1, 0, d - k + 1)$, provided that $k > 0$. The apex of these cones are represented as bigger circles in Figure 13.

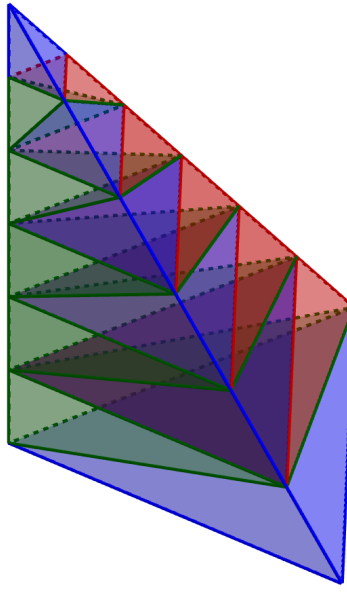
Finally, refine the join of the two segments $[(0, 0, d - 2l), (0, 2l, d - 2l)]$ and $[(0, 0, d - 2l - 1), (2l + 1, 0, d - 2l - 1)]$, provided that $0 \leq 2l < d$, and the join of the two segments $[(0, 0, d - 2l), (0, 2l, d - 2l)]$ and $[(0, 0, d - 2l + 1), (2l - 1, 0, d - 2l + 1)]$, provided that $0 < 2l \leq d$, in the unique unimodular triangulation.

The result is a unimodular triangulation Γ of Δ .

This type of floor triangulation have been used in [Dem24] and [Ite97] for constructing maximal T-surface in dimension 3. It has also been generalized in [IV07] for constructing asymptotically maximal T-hypersurface in any dimension. In particular, they showed that the triangulation Γ is convex.

6.2. Parity code, coloring and orientation. To each integer v vertex of Δ of coordinate $(x, y, z) \in \mathbb{Z}^3$ we assign a *parity code* $p(v) \in \{1, 2, 3, 4, 5, 6, 7, 8\}$, depending on the parity of x, y and z , using Table 2. These parity codes are represented in the Figure 13.

For example $v = (0, 0, 0)$ has parity code $p(v) = 2$ if d is even, and $p(v) = 4$ if d is odd.

FIGURE 14. The floor triangulation of Δ

x	y	$d - z$	parity code	sign
odd	odd	even	1	-
even	even	even	2	+
even	odd	even	3	-
even	even	odd	4	+
odd	even	even	5	-
odd	even	odd	6	+
even	odd	odd	7	-
odd	odd	odd	8	+

TABLE 2. Parity code of the vertices

We give an orientation \mathcal{O} of the edges $F_1(\Gamma)$ by the following rule. Consider an edge of Γ with vertices a and b . Since Γ is unimodular, a and b have distinct parity codes $p(a) = i$ and $p(b) = j$. We orient the edge from a to b if and only if $i > j$, and from b to a otherwise. This orientation \mathcal{O} is globally acyclic because a non-trivial oriented path necessarily joins a vertex of parity code i to a vertex of parity code j with $i > j$.

We define the sign distribution μ as follows. A vertex $a \in F_0(\Gamma)$ of parity code $p(a) = i$ has a sign $\mu(a) = +1$ if i is even and $\mu(a) = -1$ if i is odd. See Table 2.

The information about the configuration is summarized in Figure 13. Each vertex is colored according to the sign distribution and numbered by its parity code.

Let us denote $S_d = X_{\mathcal{E}_\mu \cap \mathcal{O}} \mathcal{E}_\mu$ the T-curve and $\Sigma_d = X_{\mathcal{E}_\mu}$ the T-surface obtained by patchwork.

Theorem 6.1. *There are two real algebraic hypersurfaces H_1, H_2 of degree d in $\mathbb{R}P^3$ such that the triples $(\mathbb{R}P^3, H_i, H_1 \cap H_2)$ is homeomorphic to $(\tilde{\Delta}, \Sigma_d, C_d)$, for any $i = 1, 2$.*

Proof. Since Γ is convex and \mathcal{O} is globally acyclic, we can apply the Theorem 5.6. \square

The surface Σ_d is a particular case of T-hypersurfaces studied by Itenberg:

Proposition 6.2 ([Ite97]). *The T-surface Σ_d is maximal. Its connected components are all, except one, homeomorphic to a sphere.*

A different proof of the maximality of Σ_d is given in [Dem24, section 2.1].

Our goal is to show the following result:

Theorem 6.3. *The T-curve C_d is maximal.*

6.3. Connected components of C_d . By the formula (4), the T-curve C_d is maximal if it has $d^3 - 2d^2 + 2$ connected components. All these connected components are cycles homeomorphic to circles. In the following part, we enumerate the cycles of C_d .

6.3.1. Horizontal cycles. Let v_0 be an interior vertex of T_k and let $v_1 \in F_0(\Gamma)$ be an adjacent vertex of v_0 lying outside T_k . Denote i_0 and i_1 the parities of v_0 and v_1 respectively.

Consider the star $St(v_0, v_1)$ of the edge $[v_0, v_1]$. This star contains four other vertices with two distinct parity codes. We denote them i_2 and i_3 , with $i_2 < i_3$. Observe that there are eight possible quadruplets of parities (i_0, i_1, i_2, i_3) (entirely determined by i_0): $(1,7,2,3)$, $(2,7,3,5)$, $(3,7,1,2)$, $(4,2,6,7)$, $(5,7,2,3)$, $(6,2,7,8)$, $(7,2,4,6)$ or $(8,2,6,7)$. For any of these possibilities, we can apply the proposition 5.12 to find an octant s where the axis of C_d in all the four tetrahedron of $s(St(v_0, v_1))$ is $s([v_0, v_1])$. Thus, in the octant s , the T-curve C_d contains a cycle around $[s(v_0), s(v_1)]$. See Figure 15.

If v_0 lies in the interior of T_k , with $2 \leq k \leq d-1$, there are two choices for v_1 (one in T_{k-1} and one in T_{k+1}). If v_0 lies in the interior of T_d , there is only one choice for v_1 (in T_{d-1}). Hence, the total number of horizontal cycles is

$$\sum_{k=2}^{d-1} 2 \binom{k-1}{2} + \binom{d-1}{2} = \frac{1}{3}d^3 - \frac{3}{2}d^2 + \frac{13}{6}d - 1.$$

6.3.2. Transversal cycles. Let v_0 be a vertex in the interior of S_k^l and let v_1 be an adjacent vertex of v_0 inside S_k^{l+1} . Denote i_0 and i_1 the parities of v_0 and v_1 respectively.

Consider the star $St(v_0, v_1)$ of the edge $[v_0, v_1]$. This star contains four other vertices with two distinct parities i_2 and i_3 , with $i_2 < i_3$. Observe that there are eight possible quadruplets of parities (i_0, i_1, i_2, i_3) (entirely determined by i_0): $(1,2,3,7)$, $(2,3,5,7)$, $(3,2,1,7)$, $(4,6,2,7)$, $(5,3,2,7)$, $(6,7,2,8)$, $(7,6,2,4)$ or $(8,7,2,6)$. For any of these possibilities, we can apply the proposition 5.12 to find an octant s where the axis of C_d in all the four tetrahedron of the $s(St(v_0, v_1))$ is $s([v_0, v_1])$. Thus, in the octant s , C_d contains a cycle around $[s(v_0), s(v_1)]$. See Figure 16.

If v_0 lies in the interior of S_k^l , with $1 \leq k \leq d-1$ and $1 \leq l \leq k-1$, there are two choices for v_1 (one in S_k^{l-1} and one in S_k^{l+1}). If v_0 lies in the interior of S_k^k , with

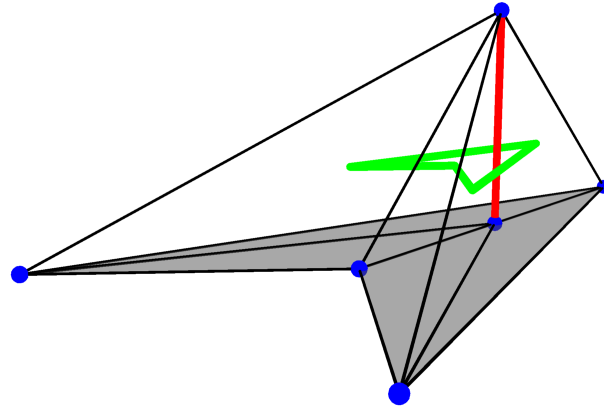


FIGURE 15. A horizontal cycle

The cycle is in green. The grey surface is a portion of a symmetric copy of T_k . The blue dots are the relevant vertices of $\tilde{\Gamma}$. The different axis of the cycle are colored in red.

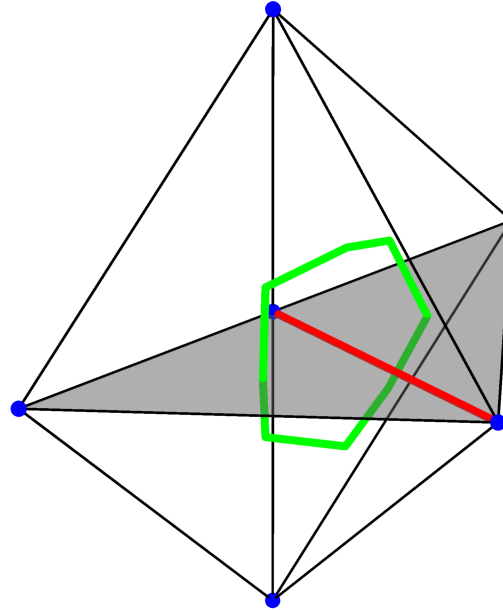


FIGURE 16. A transversal cycle

$1 \leq k \leq d-1$, there is only one choice for v_1 (in S_k^{k-1}). Hence, the total number of transversal cycle is

$$\sum_{k=1}^{d-1} \sum_{l=1}^{k-1} 2(l-1) + \sum_{k=1}^{d-1} (k-1) = \frac{1}{3}d^3 - \frac{3}{2}d^2 + \frac{13}{6}d - 1.$$

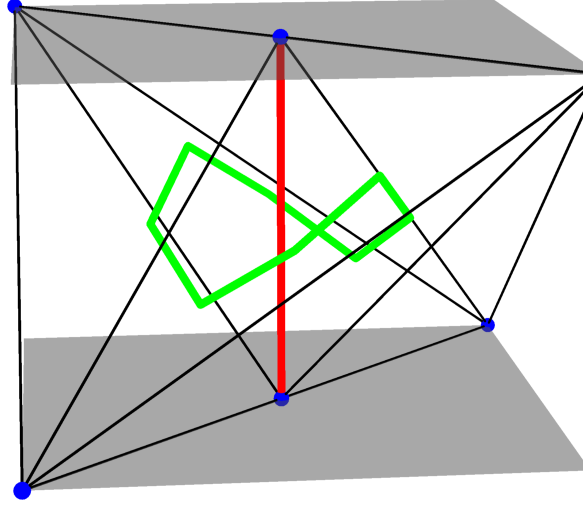


FIGURE 17. A pure join cycle

6.3.3. *Pure join cycles.* Let v_0 be an interior vertex of S_k^k (for $0 \leq k \leq d-1$) and let v_1 be an interior vertex of S_{k+1}^{k+1} . These two vertices form an edge of Γ . Denote i_0 and i_1 the parities of v_0 and v_1 respectively.

Consider the star $St(v_0, v_1)$ of the edge $[v_0, v_1]$. This star contains four other vertices and four tetrahedra. For every tetrahedron of $St(v_0, v_1)$, the set of parities of the vertices is always $\{2, 4, 5, 7\}$ and the pair $\{i_0, i_1\}$ is one of the four possibilities: $\{2, 4\}$, $\{2, 7\}$, $\{5, 4\}$ or $\{5, 7\}$. For any of these possibilities, we can apply the proposition 5.12 to find an octant s where the axis of C_d in all the four tetrahedron of $s(St(v_0, v_1))$ is $s([v_0, v_1])$. Thus, in the octant s , C_d contains a cycle around $[s(v_0), s(v_1)]$. See Figure 17.

Since S_k^k contains $k-1$ interior vertices and S_{k+1}^{k+1} contains k interior vertices, the total number of pure join cycles is

$$\sum_{k=0}^{d-1} k(k-1) = \frac{1}{3}d^3 - d^2 + \frac{2}{3}d.$$

6.3.4. *Boundary join cycles.* These cycles are similar in nature to pure join cycles, but one of their vertices lies at the cone point of the triangulation rather than strictly inside the join.

Let v_0 be an interior vertex of S_k^k and v_1 be the extremity of S_{k+1}^{k+1} on which the cone was taken in the triangulation Γ . Denote by i_0 and i_1 the parities of v_0 and v_1 , respectively.

Consider the star $St(v_0, v_1)$ of the edge $[v_0, v_1]$. This star contains four other vertices:

- v_2 and v_3 inside S_k^k both of parity code i_2
- v_4 in S_{k+1}^{k+1} of parity code i_3
- v_5 an extremity of S_{k+1}^{k+1} of parity code i_4 .

The star $St(v_0, v_1)$ is the union of four tetrahedra: $[v_0, v_1, v_2, v_4]$, $[v_0, v_1, v_2, v_5]$, $[v_0, v_1, v_3, v_4]$ and $[v_0, v_1, v_3, v_5]$.

There are four possible quintuplets of parities $(i_0, i_1, i_2, i_3, i_4)$ (entirely determined by i_0): $(2,7,5,4,3)$, $(5,7,2,4,3)$, $(4,2,7,5,6)$ or $(7,2,4,5,6)$.

In each case there exists an octant s where the axis of C_d in all the four tetrahedra of $s(St(v_0, v_1))$ is $s([v_0, v_1])$. These octants are, respectively $s = (+, +, -)$, $(+, -, +)$, $(-, +, -)$ and $(+, +, -)$. Thus, there is always an octant s such that the curve C_d form a cycle around the edge $[s(v_0), s(v_1)]$. See Figure 18

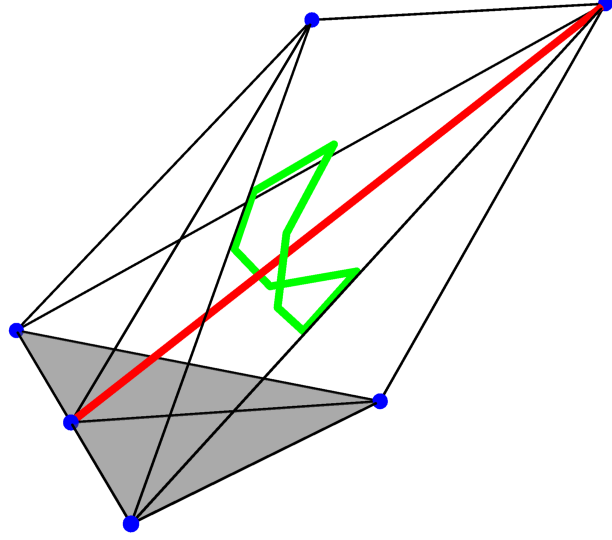


FIGURE 18. A boundary join cycle

If v_0 lies in the interior of S_k^k , with $2 \leq k \leq d-1$, there are two choices for v_1 (one in S_{k+1}^{k+1} and one in S_{k-1}^{k-1}). If v_0 lies in the interior S_d^d there is only one choice for v_1 (in S_{d-1}^{d-1}). Hence, the total number of such cycles is

$$\sum_{k=2}^{d-1} 2(k-1) + (d-1) = d^2 - 2d + 1.$$

6.3.5. Axisless cycles. Let v_0 be an extremity of S_k^l with $1 \leq l \leq k-1$. Denote F the facet of Δ containing v_0 and i_0 the parity of v_0 . We distinguish three cases:

Case A. v_0 has exactly three neighbors inside T_k .

In $\bar{\Gamma}$, the star of v_0 consists of eight tetrahedra and six other vertices:

- the two vertices of $S_k^{l\pm 1}$ adjacent to v_0 . Denote by i_1 their parity code.
- the two vertices of $T_{k\pm 1}$ adjacent to v_0 . Denote by i_2 their parity code.
- the vertex of S_k^k adjacent to v_0 and its copy along the facet F of Δ . Denote by i_3 their parity code.

There are four possible quadruplets of parities (i_0, i_1, i_2, i_3) : $(1, 2, 7, 3)$, $(2, 3, 7, 5)$, $(4, 6, 2, 7)$ or $(6, 7, 2, 8)$. In each case there is a pair of octants $\{s, s' = s + e_F\}$

where a cycle of C_d is contained in the star $St(s(v_0))$ of $s(v_0)$ in $\tilde{\Gamma}$. See Figure 19. Observe that since $v_0 \in F$, $s(v_0) = s'(v_0)$. The pair of octants is respectively $\{(+, +, -), (-, -, +)\}$, $\{(+, +, +), (-, +, +)\}$, $\{(-, +, -), (-, -, -)\}$ or $\{(+, +, -), (-, -, +)\}$.

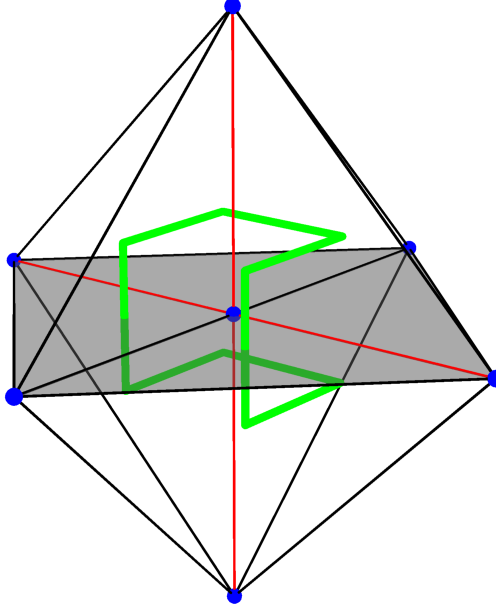


FIGURE 19. An axisless cycle of type A

Case B. v_0 has at least four neighbors inside T_k and $l \neq 1$.

Let:

- v_1 the vertex of S_k^l adjacent to v_0 , with parity code i_1
- v_2 (resp. v_5) the vertex of S_k^{l-1} (resp. S_k^{l+1}) adjacent to v_0 and v_1 , with parity code i_2
- v_3 (resp. v_6) the vertex of S_k^{l-1} (resp. S_k^{l+1}) adjacent to v_2 (resp. v_4), with parity code i_3
- v_4 (resp. v_7) the vertex of T_{k-1} (resp. T_{k+1}) adjacent to v_0 with parity code i_4 .

There are four possible quintuplets of parities $(i_0, i_1, i_2, i_3, i_4)$: $(2, 5, 3, 1, 7)$, $(3, 1, 2, 5, 7)$, $(6, 8, 7, 4, 2)$ or $(7, 4, 6, 8, 2)$. In each case there is an octant $s \in \mathcal{Q}^3$ where a cycle of C_d in the full subcomplex of $\tilde{\Gamma}$ defined by the vertices $s(v_i)$, $0 \leq i \leq 7$. See Figure 20. These octants are respectively $s = (+, +, -)$, $(-, +, -)$, $(-, -, +)$ and $(+, +, -)$.

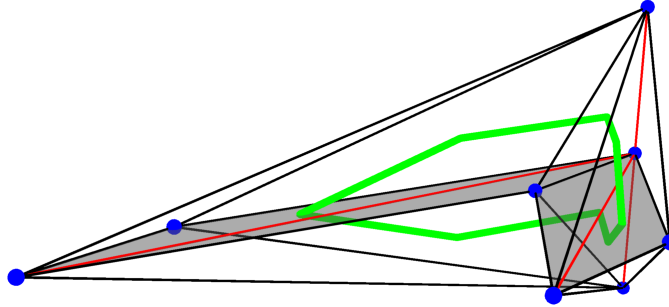


FIGURE 20. An axisless cycle of type B

Case C. The remaining case is when v_0 is the extremity of S_k^1 , having five neighbors in T_k . The parity code of v_0 is either 3 or 7. Let:

- v_1 be the unique vertex of S_k^0 ,
- v_2 be the other extremity of S_k^1 ,
- v_3 and v_4 be the two vertices of S_k^2 not on the same edge of T_k than v_0 and v_1 ,
- v_5 (resp. v_6) be the vertex of T_{k-1} (resp. T_{k+1}) neighbor of the v_i , $0 \leq i \leq 4$.

Denote by F the face of Δ containing v_0, v_1, v_5 and v_6 . For an octant $s \in \mathcal{Q}^3$, let \mathcal{H}_s be the full subcomplex of $\tilde{\Gamma}$ of the seven vertices $s(v_0) = s'(v_0), s(v_1) = s'(v_1), s(v_2), s'(v_2), s(v_3), s(v_4), s(v_5) = s'(v_5)$ and $s(v_6) = s'(v_6)$. There exists an orthant s such that C_d contains a unique cycle passing through every tetrahedron in \mathcal{H}_s . See Figure 21. The couple of octants (s, s') is $((-, +, -), (+, +, -))$ if $p(v_0) = 3$ and $((+, +, -), (+, +, +))$ if $p(v_0) = 7$.

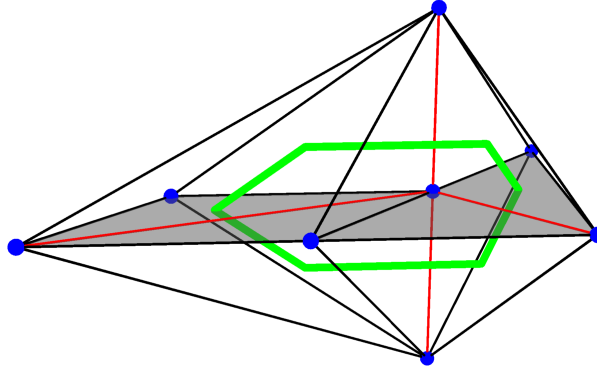


FIGURE 21. An axisless cycle of type C

Combining cases A, B and C, we have described a cycle for each extremity of S_k^l with $1 \leq l \leq k-1$ and $2 \leq k \leq d-1$. Thus, the total number of such cycles is

$$\sum_{k=2}^{d-1} \sum_{l=1}^{k-1} 2 = (d-1)(d-2) = d^2 - 3d + 2.$$

6.3.6. *The last cycle.* There is one additional cycle, not localized in a small number of simplices.

This cycle can be detected by observing that, none of the previously described cycles pass through a copy of T_0 . But all interior faces must have exactly two copies intersecting C_d , this implies the existence of an additional cycle.

6.3.7. *Conclusion.* If we add up all the cycles we have described we obtain a total of

$$d^3 - 2d^2 + 2$$

distinct cycles. So $b_0(C_d) \geq d^3 - 2d^2 + 2$. Thus, C_d is maximal. This completes the proof of the Theorem 6.3.

6.4. Concluding remarks.

Remark 6.4. By construction, we have the inclusion $C_d \subset \Sigma_d$. Being careful, it is possible to describe the topology of the embedding of C_d in Σ_d . For instance, consider the star of an interior vertex of parity code 3 in the orthant $(-, -, -)$. In this star, the T-surface Σ_d has one spherical component enclosing the vertex of parity code 3, while the T-curve C_d has exactly two horizontal cycles lying in this sphere. The situation is represented in Figure 22. This shows that the connected components of C_d are distributed between different components of Σ_d , and do not all belong to a single one.

In particular, consider the real algebraic surface \mathcal{S}_d and curve \mathcal{C}_d corresponding respectively to Σ_d and C_d , by Theorem 5.6. Then, the spreading of the connected components of $\mathbb{R}\mathcal{C}_d$ in multiple components of $\mathbb{R}\mathcal{C}_d$ implies that the pair $(\mathcal{S}_d, \mathcal{C}_d)$ is not maximal in the sense of Smith-Thom inequality:

$$\sum_i \dim H_i(\mathbb{R}\mathcal{S}_d, \mathbb{R}\mathcal{C}_d; \mathbb{F}_2) < \sum_i \dim H_i(\mathbb{C}\mathcal{S}_d, \mathbb{C}\mathcal{C}_d; \mathbb{F}_2)$$

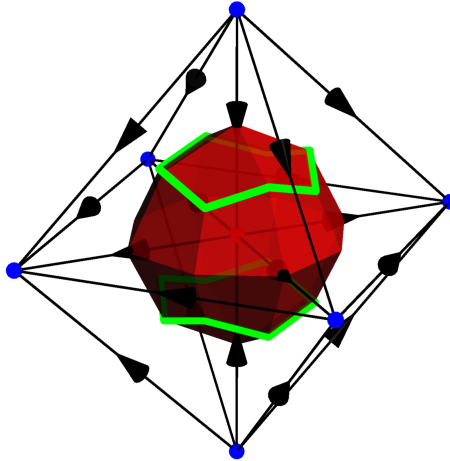


FIGURE 22. A component of the T-surface (in red) containing two cycles of the T-curve (in green)

Remark 6.5. The triangulation Γ possesses the special property that every tetrahedron has, at least, an edge on the boundary of Δ . This condition is crucial: by an argument similar to the proof of Theorem 4.5, any tetrahedron lacking such a boundary edge yields a subdivision of K_5 in the dual graph G_Γ and consequently prevents the existence of a maximal T-curve. We think families of triangulations of dilations of 3-polytopes sharing this property are rare.

For example, consider Δ the pyramid over a Nakajima polygon defined as the convex hull of the vertices $(0, 0, 0)$, $(0, \mu, 0)$, $(\lambda, \mu, 0)$, $(\lambda + \alpha\mu, 0, 0)$ and $(0, 0, 1)$, where α, λ, μ natural numbers such that $\lambda, \mu \neq 0$. Bertrand ([Ber02, chapter 8]) constructed maximal real algebraic curves in $\mathbb{R}X_\Delta$ using Sturmfels' patchworking method (rather than via real phase structure).

The dilation $d\Delta$ of Δ can be triangulated in the same fashion as for $d\Delta_3$ by slicing it horizontally. See Figure 23. However, for any choice of apex for the cone over a slice, one inevitably creates tetrahedra without any boundary edge (in green on Figure 23).

Thus, our construction cannot be directly extended to Δ to obtain maximal T-curve.

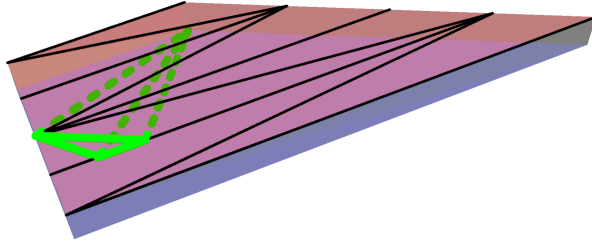


FIGURE 23. The triangulation between two slices of Nakajima polygons, with in green a tetrahedron with no boundary edge in the whole pyramid

REFERENCES

- [BBR17] B. Bertrand, E. Brugallé, and A. Renaudineau. Haas' theorem revisited. *Epjournal de géométrie algébrique*, Volume 1, 2017.
- [Ber02] B. Bertrand. *Hypersurfaces et intersections complètes dans les variétés toriques*. PhD thesis, Université de Rennes 1, 2002.
- [Bih02] F. Bihan. Viro method for the construction of real complete intersections. *Adv. Math.*, 169(2):177–186, 2002.
- [BLdMR24] E. Brugallé, L. López de Medrano, and J. Rau. Combinatorial patchworking: Back from tropical geometry. *Transactions of the American Mathematical Society*, 377(10):6793–6826, 2024.
- [BLVS⁺99] A. Björner, M. Las Vergnas, B. Sturmfels, N. White, and G. Ziegler. *Oriented matroids*, volume 46. Cambridge University Press, second edition, 1999.
- [BR15] M. Beck and S. Robins. *Computing the Continuous Discretely*. Springer New York, NY, 2015.

- [Bro62] M. Brown. Locally flat imbeddings of topological manifolds. *Annals of Mathematics*, 75(2):331–341, 1962.
- [CLS11] D. Cox, J. Little, and H. Schenck. *Toric varieties*. Providence, RI: American Mathematical Society (AMS), 2011.
- [Dem24] A. Demory. *Constructions of three- and four-dimensional real algebraic varieties*. PhD thesis, Sorbonne Université, 2024.
- [DLRS10] J. De Loera, J. Rambau, and F. Santos. *Triangulations: structures for algorithms and applications*, volume 25. Springer Science & Business Media, 2010.
- [FL78] J. Folkman and J. Lawrence. Oriented matroids. *Journal of Combinatorial Theory, Series B*, 25(2):199–236, 1978.
- [GKZ08] I.M. Gelfand, M. Kapranov, and A. Zelevinsky. *Discriminants, Resultants, and Multidimensional Determinants*. Modern Birkhäuser Classics. Birkhäuser Boston, 2008.
- [Haa97] B. Haas. *Real algebraic curves and combinatorial constructions*. PhD thesis, Université de Strasbourg, 1997.
- [Ite93] I. Itenberg. Contre-exemples à la conjecture de ragsdale. *Comptes Rendus-Académie Des Sciences Paris SERIE 1*, 317:277–277, 1993.
- [Ite95] I. Itenberg. Counter-examples to Ragsdale conjecture and T-curves. In *Real algebraic geometry and topology (East Lansing, MI, 1993)*, volume 182 of *Contemp. Math.*, pages 55–72. Amer. Math. Soc., Providence, RI, 1995.
- [Ite97] I. Itenberg. Topology of real algebraic T-surfaces. *Revista Matemática de la Universidad Complutense de Madrid*, 10(Supl.):131–152, 1997.
- [IV96] I. Itenberg and O. Viro. Patchworking algebraic curves disproves the ragsdale conjecture. *Math. Intelligencer*, 18(4):19–28, 1996.
- [IV07] I. Itenberg and O. Viro. Asymptotically maximal real algebraic hypersurfaces of projective space. In *Proceedings of Gökova Geometry-Topology Conference 2006*, pages 91–105. Gökova Geometry/Topology Conference (GGT), Gökova, 2007.
- [Kho78] A. G. Khovanskii. Newton polyhedra and the genus of complete intersections. *Functional Analysis and Its Applications*, 12:38–46, 1978.
- [Kle76] F. Klein. Ueber eine neue art von riemann'schen flächen. *Mathematische Annalen*, 10:398–416, 1876.
- [MS15] D. Maclagan and B. Sturmfels. *Introduction to Tropical Geometry*. AMS, 2015.
- [New60] M. H. A. Newman. On the division of euclidean n -space by topological $(n - 1)$ -spheres. *Proceedings of the Royal Society of London. A. Mathematical and Physical Sciences*, 257(1288):1–12, 08 1960.
- [Ris92] J.-J. Risler. Constructions d'hypersurfaces réelles [d'après Viro]. *Séminaire Bourbaki*, 1992.
- [RRS22] J. Rau, A. Renaudineau, and K. Shaw. Real phase structures on matroid fans and matroid orientations. *Journal of the London Mathematical Society*, 106(4):3687–3710, 2022.
- [RRS25] J. Rau, A. Renaudineau, and K. Shaw. Real phase structures on tropical varieties and patchworks in higher codimension. *International Mathematics Research Notices*, 2025(20):rnaf312, 10 2025.

- [RS23] A. Renaudineau and K. Shaw. Bounding the Betti numbers of real hypersurfaces near the tropical limit. *Ann. Sci. Éc. Norm. Supér. (4)*, 56(3):945–980, 2023.
- [Stu94] B. Sturmfels. Viro’s theorem for complete intersections. *Annali della Scuola Normale Superiore di Pisa-Classe di Scienze*, 21(3):377–386, 1994.
- [Tho81] C. Thomassen. Kuratowski’s theorem. *Journal of Graph Theory*, 5(3):225–241, 1981.
- [Vir84] O. Viro. Gluing of plane real algebraic curves and constructions of curves of degrees 6 and 7. In Ludwig D. Faddeev and Arkadii A. Mal’cev, editors, *Topology*, pages 187–200, Berlin, Heidelberg, 1984. Springer Berlin Heidelberg.
- [Vir01] O. Viro. Dequantization of real algebraic geometry in a logarithmic paper. In Birkhauser, editor, *Proceedings of the 3rd European Congress of Mathematicians*, 2001.
- [Vir06] O. Viro. Patchworking real algebraic varieties. <https://arxiv.org/abs/math/0611382>, 2006.